

Final Technical Report

A Heterogeneous System for Eagle Detection, Deterrent, and Wildlife Collision Detection for Wind Turbines

Recipient Organization: Oregon State University, Corvallis, OR, USA
DOE Award Number: DE-EE0007885
Project Period: 04/01/2017 - 07/01/2020
Date of Last Revision: January 22, 2021

Principal Investigators:

- Roberto Albertani, Associate Professor, School of Mechanical, Industrial and Manufacturing Engineering, Oregon State University
- Matthew L. Johnston, Associate Professor, School of Electrical Engineering and Computer Science, Oregon State University

Research Partners:

- Kyle Clocker, School of Electrical Engineering and Computer Science, Oregon State University
- Congcong Hu, School of Mechanical, Industrial and Manufacturing Engineering, Oregon State University
- Manuela Huso, USGS Forest and Rangeland Ecosystem Science Center
- Todd Katzner, USGS Forest & Rangeland Ecosystem Science Center
- William Maurer, School of Mechanical, Industrial and Manufacturing Engineering, Oregon State University
- Sinisa Todorovic, Professor, School of Electrical Engineering and Computer Science, Oregon State University
- Johnny Vang, School of Mechanical, Industrial and Manufacturing Engineering, Oregon State University

Acknowledgment: This material is based upon work supported by the U.S. Department of Energy's Office of Energy Efficiency and Renewable Energy (EERE) under the Wind Energy Technologies Office Award Number DE-EE0007885.

Disclaimer: This report was prepared as an account of work sponsored by an agency of the United States Government. Neither the United States Government nor any agency thereof, nor any of their employees, makes any warranty, express or implied, or assumes any legal liability or responsibility for the accuracy, completeness, or usefulness of any information, apparatus, product, or process disclosed, or represents that its use would not infringe privately owned rights. Reference herein to any specific commercial product, process, or service by trade name, trademark, manufacturer, or otherwise does not necessarily constitute or imply its endorsement, recommendation, or favoring by the United States Government or any agency thereof. The views and opinions of authors expressed herein do not necessarily state or reflect those of the United States Government or any agency thereof.

Executive Summary

Continued development, expansion, and operation of wind energy installations must be managed in conjunction with effects on local wildlife, with special attention paid to protected avian and bat species that may be affected by wind turbine collisions [1]. Ongoing efforts to measure and mitigate wind turbine impacts on wildlife include improved pre-construction siting and post-construction monitoring, development of deterrent technologies and curtailment strategies, and improved quantitative assessment of wildlife mortality due to wind turbines [2]–[4].

This report summarizes the design, implementation, and test of an integrated system for automated detection and deterrence of eagles, with included wind turbine blade strike detection and imaging functionality. A machine learning approach was used in conjunction with a 360° camera system for automated detection and classification of golden eagles. This was developed using footage obtained from trained golden eagles and other raptors, in collaboration with wildlife biologists and professional bird handlers. Oregon State University developed a visual deterrent system, which uses inflatable anthropomorphic sculptures with random, kinetic motion to deter eagles, and conducted limited field testing on live eagles; the deterrent can be triggered by the visual detection of eagles using the vision system. Finally, a multi-sensor module was developed that is mounted at the turbine blade root. This module measures vibration and other motions to detect blade strikes, and an integrated on-blade camera captures an image of any impacting objects. Long-term, this blade strike detection system is intended to support an automatic monitoring and certification system for the eagle detection and deterrent system. Independent field testing of each system component is described.

Visual eagle detection testing was done in collaboration with the High Desert Museum in Bend, OR using trained birds, including both eagles and other raptors. The final eagle classification algorithm (eagle/non-eagle) had a per-frame accuracy of 91.54% using the 360° 4K camera.

Visual deterrent testing was conducted in two field tests with wild eagles near Klamath Falls, OR. The deterrent was deployed from the ground when an eagle flies overhead, and observers noted any perceived change in flight trajectory. Interactions were also recorded on video. Results were overall inconclusive due to the small number of eagles that were close enough to the field test for observed interactions.

Testing of the integrated system on an operational wind turbine was conducted across three separate field tests. This includes multi-day field tests on a General Electric 1.5MW wind turbine at the National Renewable Energy Laboratory (NREL) National Wind Technology Center (NWTC) in Boulder, CO in October 2018 and July 2019; installation procedures, test procedures, and a summary of collected data are presented. A third multi-day on-turbine field test is also presented, which was performed using a General Electric 1.5MW wind turbine at the North American Wind Research and Training Center (NAWRTC) at Mesalands Community College, Tucumcari, NM in April 2019. Across these field tests, the vision system was demonstrated using unmanned aerial vehicles (UAV), and the eagle classification algorithm was not tested; the visual deterrent system was demonstrated, including automatic, remote deployment following surrogate visual detections; and, multi-sensor on-blade data was recorded across multiple wind turbine operational conditions and through more than 100 surrogate blade strikes using soft projectiles, including the successful demonstration of automatic image capture of striking objects. This data set was also used for offline development and validation of enhanced collision detection algorithms.

As summarized in this report, the development and field validation of an integrated detection, deterrent, and blade collision detection system represents a critical proof of concept for future technology development of related detection and deterrent technologies, where both deterrent as well as collision detection recording devices are needed for future siting, monitoring, and operation of wind turbine installations, both onshore and offshore.

A Heterogeneous System for Eagle Detection, Deterrent, and Wildlife Collision Detection for Wind Turbines

Final Technical Report

DE-0007885

Table of Contents

EXECUTIVE SUMMARY	2
1. PROJECT OVERVIEW	4
2. SUMMARY OF TECHNICAL OBJECTIVES AND SYSTEM COMPONENTS	6
2.1. <i>Eagle Detection System using 360° Imaging and Machine Learning (Task 1.00)</i>	6
2.2. <i>Eagle Deterrent System using Kinetic Visual Deterrent (Task 2.00)</i>	10
2.3. <i>Blade Collision Detection System with On-Blade Image Capture (Task 3.00)</i>	14
2.4. <i>System Integration and Full System Testing (Task 4.00)</i>	17
3. SUMMARY OF FIELD TESTING (TASK 5.00)	20
3.1. <i>Field Testing at NREL-NWTC, Boulder, CO – October 2018</i>	20
3.2. <i>Field Testing at Mesalands Community College, Tucumcari, NM – April 2019</i>	25
3.3. <i>Field Testing at NREL-NWTC, Boulder, CO – July 2019</i>	29
3.4. <i>Development of automated collision detection algorithms</i>	32
4. CONCLUSIONS AND SUGGESTED FUTURE WORK	34
4.1. <i>Automated Visual Detection of Eagles:</i>	34
4.2. <i>Visual Deterrent using Kinetic Humanoid Devices:</i>	34
4.3. <i>Automated Blade-Strike Collision Detection:</i>	34
4.4. <i>Ongoing Work using Recorded Data Sets from On-Turbine Testing:</i>	35
5. SUMMARY OF PROJECT OUTCOMES (TASK 6.0)	35
5.1. <i>Presentations</i>	35
5.2. <i>Peer-Reviewed Publications / Proceedings</i>	36
5.3. <i>Intellectual Property</i>	36
5.4. <i>Demonstrations</i>	36
5.5. <i>Media</i>	36
6. ACKNOWLEDGMENTS	37
7. REFERENCES	37

1. Project Overview

Continued development, expansion, and operation of wind energy installations must be managed in conjunction with effects on local wildlife, with special attention paid to protected avian and bat species that may be affected by wind turbine collisions [1]. Ongoing efforts to measure and mitigate wind turbine impacts on wildlife include improved pre-construction siting and post-construction monitoring, development of deterrent technologies and curtailment strategies, and improved quantitative assessment of wildlife mortality due to wind turbines [2]–[4]. Building energy infrastructure that minimized negative impacts to wildlife safety is a key concern. The broad mission for this project is to improve technologies that will protect eagles sharing airspace with wind turbines by providing wind energy operators with cost-effective technologies for reducing the impact of wind turbines on eagles and other species.

Bald and golden eagles are protected under the Bald and Golden Eagle Protection Act (BGEPA), and wind facilities must comply with state and federal laws protecting wildlife both for siting and for ongoing regulatory compliance. Moreover, developers and operators of wind energy facilities often must take measures to mitigate the potential impacts of their facilities on protected species. To address this problem, the present project is developing a system designed to automatically detect and classify eagles, with the intent of triggering a deterrent device to scare eagles away from turbine blades. An on-blade system is also incorporated for detecting and image capture of any objects colliding with a turbine blade.

Three fundamental objectives were addressed through this project: 1) detection of eagles flying in proximity of wind turbines using automated image classification, 2) eagle deterrence using inflatable ground-based kinetic visual deterrents, and 3) automated blade collision detection and on-blade image capture for continuous monitoring of potential blade strikes. The latter addresses the fundamental needs of eagle impact minimization validation without human operators.

Following the design, implementation, and standalone validation of each system component, the integrated smart sensor system was tested across two field tests on a 1.5MW GE wind turbine at the Northwest Wind

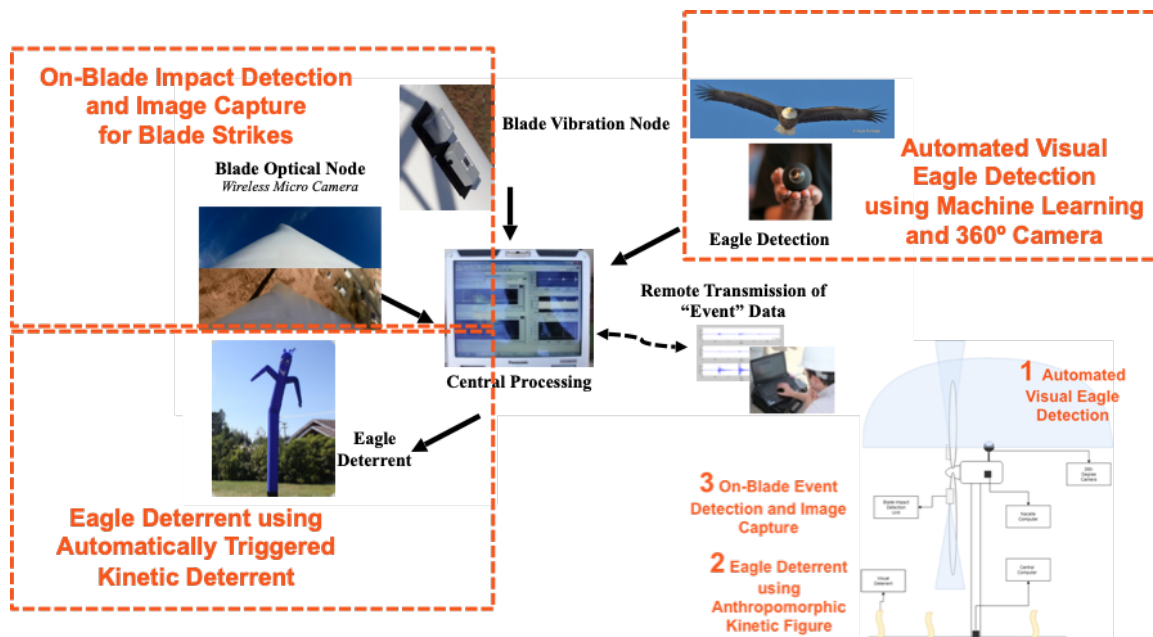


Figure 1 Overview of integrated system for visual detection of wild eagles, deterrence using a visual kinetic deterrent system, and on-blade sensor and imaging system for automated collision detection and blade strike imaging. The combined system was tested both in parts and as a complete integrated system across multiple fields tests, including testing on operational wind turbines.

Technology Center (NWTC), National Renewable Energy Laboratory, Boulder, CO, and through a third on-turbine field test at the North American Wind Research and Training Center (NAWRTC), Mesalands Community College, NM. In addition, we partnered with the High Desert Museum, Bend, OR, to generate training videos of golden eagles and other raptors, which were used for training and testing of our automated eagle detection machine vision algorithms. This extensive and collaborative testing and validation plan was essential for demonstrating a field-ready solution for detection, deterrence, and collision monitoring for wind turbines.

Across the field tests, the vision system was demonstrated using unmanned aerial vehicles (UAV); the visual deterrent system was demonstrated, including automatic deployment; and, multi-sensor on-blade data was recorded across multiple wind turbine operational conditions and through more than 100 surrogate blade strikes using soft projectiles, including the successful demonstrating automatic image capture of striking objects. This data set was also used for offline development and validation of enhance collision detection algorithms.

This report is structured to correspond to the Statement of Project Objectives organization: development and standalone testing of the eagle detection vision system (Task 1.00), development and standalone testing of the visual deterrent system (Task 2.00), development and standalone testing of the on-blade collision detection system (Task 3.00), integration and testing of the combined detection, deterrent, and collision detection system (Task 4.00), and complete system field testing with operational wind turbines (Task 5.00).

As summarized in this report, the development and field validation of an integrated detection, deterrent, and blade collision detection system represents a critical proof of concept for future technology development of related detection and deterrent technologies, where both deterrent as well as collision detection recording devices are needed for future siting, monitoring, and operation of wind turbine installations, both onshore and offshore. While designed for the detection and deterrence of golden eagles, the proposed system is broadly extensible to avian and bat species.

2. Summary of Technical Objectives and System Components

2.1. Eagle Detection System using 360° Imaging and Machine Learning (Task 1.00)

Overview and Background

A robust computer vision system was developed for detecting eagles using a 360° camera view in real time, leveraging modern machine learning approaches. The vision system is illustrated in Fig. 2 and consists of a *video capture system*, aimed at taking and streaming video footage, and software for *video processing*, aimed at detecting the moment and location an eagle appears in the field of view. The output of the vision system can be used in conjunction with other sensors for eagle detection for a timely triggering of the bird deterrents or for initiating curtailment in future systems. This section summarizes the design, training, and testing of the integrated visual detection system trained for classifying eagles.

Visual detection hardware and system design

To ensure a sufficient video resolution and wide field of view, the system was implemented using a 360° video camera with 4K resolution (Fly360). The camera captures a panoramic video with the 360-degree field of view, and a custom mounting apparatus was design for mounting the camera on the wind turbine nacelle. Initial training videos were recorded to the camera's internal memory, and a real-time remote video feed was implemented for use in the final integrated system.

Automated eagle detection algorithm overview

A unified deep-learning framework was developed for eagle detection and trajectory estimation, as illustrated in Fig. 2. The automated eagle detection and classification occurs in two stages: frame-by-frame feature extraction, and fusion of features across time intervals. The two-stage video processing is implemented using a deep-learning framework, following recent breakthroughs in computer vision and deep convolutional neural networks (CNNs). Deep CNNs have been shown as the most accurate and robust detectors of visual cues, since they are automatically trained on large datasets to achieve optimality, unlike traditional hand-designed approaches. For fusing the extracted features and final recognition, in the second

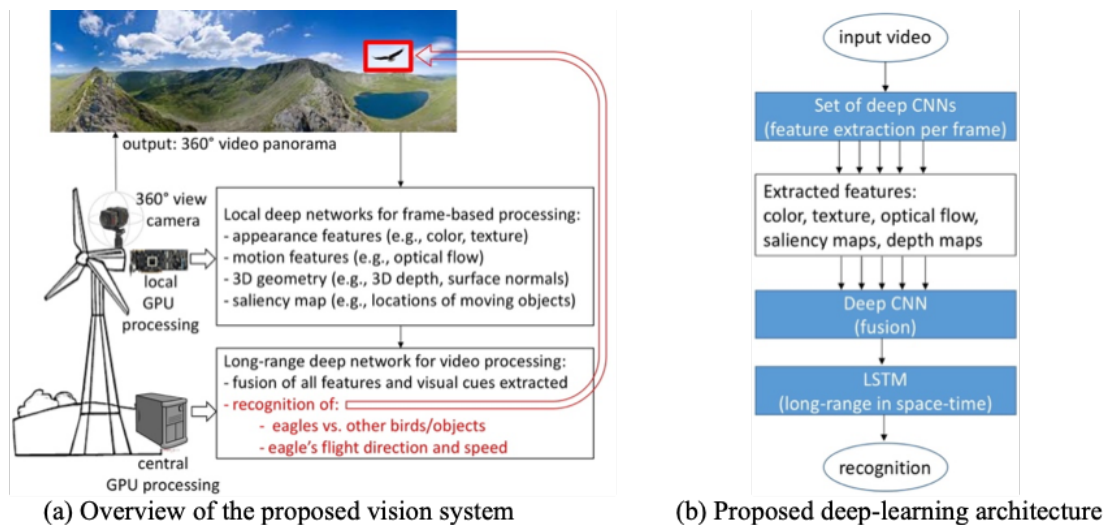


Figure 2 A 360° camera is used to capture a panoramic video. Video processing consists of two stages: feature extraction identifies important visual cues from every frame, and the results of this local processing are fused over long-range time intervals for eagle detection and trajectory estimation. The local and central video processing will be specified as a cascade of deep convolutional neural networks (CNN).

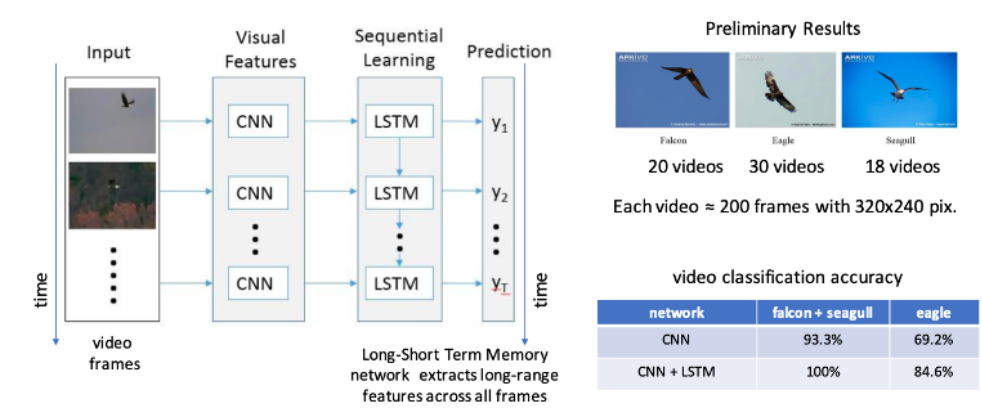


Figure 3 For initial classifier design and training, collected YouTube flight videos of three species of birds were collected, including eagles, falcons, and seagulls. We have implemented a deep neural network architecture for identifying the bird species shown in the video; the table summarizes initial video classification accuracy.

stage of video processing, we will use a deep, recurrent neural network, called Long-Short-Term Memory (LSTM). LSTMs can reliably model complex appearance and motion behaviors of various objects, due to its capability to capture long-range statistical dependencies of patterns in space and time.

Collection of training videos with trained eagles and other raptors

Initial model design, training, and validation were completed using publicly available videos of birds in flight. By using a deep neural network that will analyze videos at multiple resolutions, from fine-scale to coarse, simultaneously, our approach is therefore scale-invariant (over a wide range of video resolutions). A summary of initial model training and validation is illustrated in **Fig. 3**. A total of 68 YouTube flight videos of three species of birds was collected, including eagles, falcons, and seagulls. The videos were split into 2/3 for training and 1/3 for testing. We have implemented a deep neural network architecture for identifying the bird species shown in the video. The deep architecture consists of the convolutional neural network (CNN) for analyzing every video frame, and Long-Short Term Memory network (LSTM) for fusing CNN's outputs across all frames toward the final video classification. The CNN+LSTM architecture has been trained on the training videos, and then our classification accuracy has been estimated on the test videos. The table in **Fig. 3** shows the initial video classification accuracy.

Automated eagle detection algorithm initial training

To generate videos of eagle flights using the selected 360° camera hardware, two video recording sessions were completed using trained raptors. The first session was completed at the High Desert Museum in Bend, Oregon in August 2017. In coordination with the museum, a number of flights were recorded using trained raptors. A total of 34 videos, including seven with a golden eagle (*Aquila chrysaetos*) and 23 with other raptors (Harris's hawk, turkey vulture, barn owl, aplomado falcon, peregrine falcon) were recorded. In addition, a local master falconer works with a trained golden eagle in Vale, OR, where a recording session was conducted in September 2017. A total of 14 movies were recorded with different flight paths and backgrounds. For both recording sessions, videos were recorded using the 360° camera at a frame rate of 30 f/s and 2880x2880 pixel resolution. Several videos were recorded by two 360° cameras simultaneously.

Automated eagle detection algorithm development and training using 360° video images

Using the recorded videos, software was implemented that addresses the following problem statement: given a 360-degree video, as shown in Figure 2, automatically label each video frame with one of the two classes "eagle" and "non-eagle", where the class "eagle" is assigned to a frame if it shows a flying or static

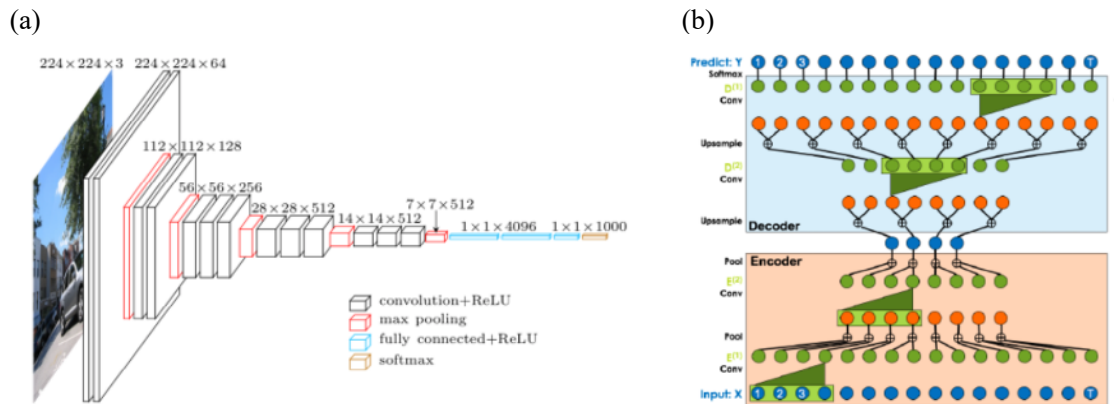


Figure 4 (a) Illustration of the deep convolutional neural network (CNN) used for extracting a 1000- dimensional deep-feature vector from every video frame. (b) Temporal convolutional neural network (TCNN). Input to the TCNN, X, are deep-feature vectors extracted from each video frame. Output of the TCNN, Y, are class labels assigned to every video frame.

eagle, and the class “non-eagle” is assigned to a frame if it does not show an eagle but either some other static or flying birds (raptors) and objects in the background.

First, video frames are processed with a deep convolutional neural network (CNN), whose numbers of convolutional filters in each layer, and the number of layers are specified in **Fig. 4a**. The CNN extracts a 1000-dimensional deep-feature vector from every video frame.

Second, the temporal sequence of CNN’s deep features extracted from video frames are input to the temporal convolutional neural network (TCNN) for labeling every frame with classes “eagle” or “non-eagle”. **Figure 4b** shows the TCNN. Note that the TCNN performs temporal segmentation of the video into intervals where an eagle is visible and intervals where an eagle is not visible.

It is worth noting that this implementation differs from the initial approach. The prior model used a Long Short-Term Memory network (LSTM) as a part of the prospective approach. However, in initial experiments, it was found that the LSTM requires significantly more training data for robust learning than is available for this application. Due to the inherent difficulty in collecting example videos of eagles, our training dataset is limited, and thus required a modification of the proposed approach. The implemented TCNN is a good alternative, as it demonstrates better performance than the LSTM in our preliminary tests.

Initial validation using all recorded videos with trained birds:

The CNN and TCNN were specifically trained to classify ‘eagle’ and ‘non-eagle,’ as defined by the problem statement above. We manually annotated every frame of 54 video clips from both field recordings, with lengths spanning 10-30 seconds, with the two classes. In our video annotation, we faced the following challenges: a) Eagles and other birds are barely visible by a human eye when flying against cluttered background (e.g., trees of a forest); consequently, ground truth about eagle appearance cannot be well-defined for such videos. (b) Manual annotation is time consuming; consequently, the sizes of training and test datasets are inherently limited, and do not meet standard requirements for robust training and testing of deep neural networks. Preliminary tests conducted during the software development demonstrated the following. Runtime is less than 0.1s per frame, which allows for real-time video processing once temporal subsampling is implemented in hardware (e.g., processing every 2nd or 3rd frame, instead of processing every frame). We used two random splits of 28 video clips for training and 26 video clips for testing and obtained the average two-class (“eagle” and “non-eagle”) frame-labeling accuracy of 89.36% and 79.47% on training and test data, respectively.

Field-specific validation using mixed raptor videos:

Specifically, the High Desert Museum field test generated 34 video clips for evaluation, in which the eagle appears in 2030 video frames and another bird raptor appears in 620 video frames, as manually annotated by our students. In these videos, distances of the eagles and other birds from the camera range approximately between 30-150 feet. Further distances of birds are not considered, since they cannot be reliably seen in the video by a human, and hence cannot be annotated. Videos of these further distances are excluded from testing and training, as ground truth cannot be established.

Following iterative improvement of the software, we evaluated our final software for eagle detection, where the goal is to correctly detect every frame in which the eagle appears vs. frames that show other bird raptors or no birds at all. Our final average per-frame eagle detection accuracy is 91.54% on the field-test videos; other results can be readily derived from the reported per-frame accuracy. This indicates that in 2426 of the combined 2650 video frames were correctly classified, and 224 were incorrectly classified (including both false positive and false negative). Our accuracy of detecting video intervals when the eagle truly appears in the video is 100%.

Detection latency and trajectory estimation:

We also evaluated our accuracy on how well we detect the start and end of a video interval when the eagle truly appears and disappears from the video. On average, our software has a delay of correct eagle detection of 4.2 video frames after the true moment when the eagle appears in the video. Also, on average, our software has a delay in detecting the true moment when the eagle disappears from the video's field-of-view of 1.5 video frames. Finally, we evaluated our software for eagle-flight trajectory estimation over the eight trajectory classes – namely, moving “left”, “right”, “up”, “down”, each modified by either “toward” or “away” from the camera. Our average accuracy of eagle-flight trajectory estimation is 93.12%.

Field-based testing of the integrated eagle detection hardware/software vision system:

In addition to development and validation of the eagle detection algorithms, the integrated vision system was demonstrated in the field including video link and on-site processing at the High Desert Museum, Bend, OR, during a video collection trip. The integrated hardware system was deployed in the field and tested, and the videos of eagles and other raptor birds were recorded using this hardware system. The following hardware components were integrated for the field test: power system, camera system, video transmission system, video-to-frame extraction storage and buffering, and GPU processor for video analysis (HP Z840 with NVIDIA Quadro M6000 GPU).

The demonstrated hardware system is capable of: recording 24 frames per second of 4K, 360-degree video; transmitting such streaming video to a stand-alone workstation; extracting and buffering frames from the streaming video at the same rate of 24 frames per second; and finally, processing the extracted video frames at a slower rate of 10 frames per second using the software for eagle detection and trajectory estimation on a GPU processor. The slower video processing rate is due to the processing times required for grabbing individual frames from the buffer and then running the eagle detection and trajectory estimation software.

The processing rate of 10 frames per second is nearly real-time, and it introduces a delay in eagle detection of less than one half of a second. This can be improved with additional computational power, or by processing a subset (e.g. every other) video frame; given that an eagle cannot occur for a single frame only, this is sufficient for the purposes of this application.

2.2. Eagle Deterrent System using Kinetic Visual Deterrent (Task 2.00)

Overview and Background

One of the most effective golden eagle depredation control measures was previously reported to be a combination of harassment and increase of human activity [5], and a related result from the 2016 NREL “Wind Energy Industry Eagle Detection and Deterrents: Research Gaps and Solutions Workshop” was that human-like figures are particularly effective in disturbing and harassing eagles [6]. As conspicuous negative visual stimuli have been shown to be the most effective method to deter eagles from flying around certain areas, we proposed and developed a deterrent system comprised of bright, inflatable kinetic devices (i.e. ‘air dancers’) to be operated on the ground to deter eagles from approaching the rotor swept area.

Although no prior data exists for eagle reactions to air dancers, a significant amount of data and practical experience are available on the effect of air dancers on other birds. Research on air dancer effectiveness to scare wild birds was funded by a three-year multi-state USDA-National Institute of Food and Agriculture Specialty Crop Initiative grant. Cornell University studies on air-dancer effectiveness concluded that vegetable-farm yield increased by 1 to 19% by using air dancers [7]. Similar results were observed in blueberry farms [8] while a West Washington study found medium to high effectiveness of air dancers operated in Pacific Northwest sweet cherries orchards to scare birds.

Toward testing this deterrent method, an integrated control and actuation system was implemented for remote activation of kinetic visual deterrents – either directly, or by integration with the automated eagle detection visual system (Task 1.00). The devices were tested in a variety of controlled conditions to assure viability at high wind velocity and over long exposure, and two limited field trials were conducted to assess the efficacy of the deterrent in the presence of wild eagles. This section summarizes the design, validation, and field testing of the visual deterrent system using kinetic air dancers.

Visual deterrent system design and implementation

Commercial kinetic inflatable devices (colloquially known as ‘skydancers’ or ‘air dancers’) consist of a fabric tube inflated by an electric fan, typically used for advertising purposes; the shape of the device leads to erratic, human-like movement of the fabric tube. Multiple devices were acquired and tested in 6ft, 10ft, and 20ft, heights; colors (orange, yellow, blue) were suggested by wildlife biologist collaborators, including Dr. Fernandez-Juricic Esteban from Purdue University; Dr. Esteban has identified blue in particular as a color highly visible by eagles considering the background of the test site. For remote activation and use in the field, an electrical system was designed to provide long range (>100m) wired and wireless activation and deactivation of the devices, as well as standalone operation from deep cycle battery or direct wired power. The system is illustrated in **Fig. 5** for initial electrical testing.

Visual deterrent laboratory testing

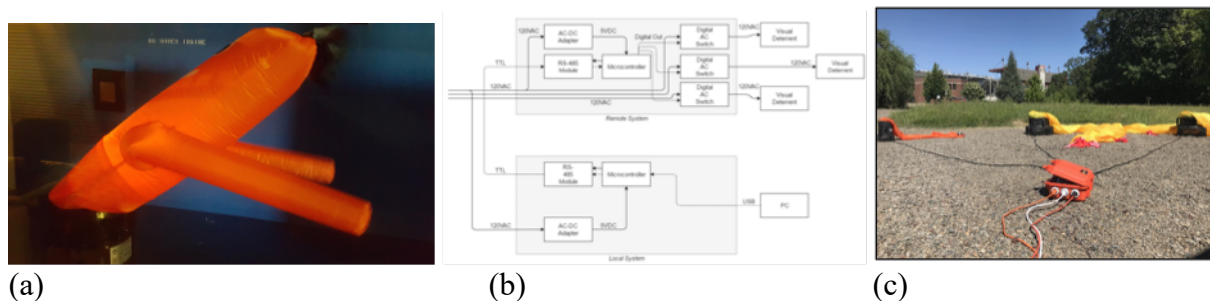


Figure 5. (a) A 6ft visual deterrent undergoing initial testing in the OSU wind tunnel; (b) a simple electrical system for power and remote activation of visual deterrents; and, (c) initial testing of the visual deterrent system.

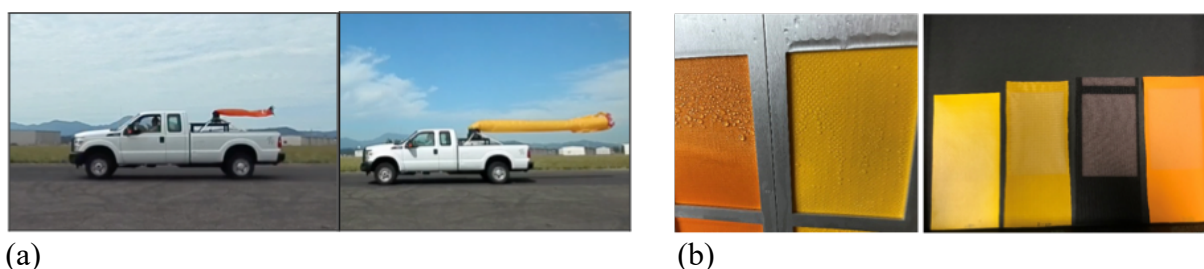


Figure 6. (a) Maximum wind velocity testing for visual deterrents Deployment at 55 mph (orange, ~25 m/s) and 45 mph (yellow, ~20 m/s) for the 6- and 20-foot variants. (b) Accelerated weather testing (AWT) of deterrent materials compared to common exterior-use waterproof-breathable fabric (orange) and tarp (yellow) materials; post-AWT samples at right.

Visual deterrents were tested in controlled settings to establish viability for use in the field at wind turbine installations. In addition to cycle testing of the integrated electrical system and preliminary wind tunnel testing (Fig. 5a), representative testing is illustrated in **Fig. 6**. In Fig. 6a, vehicle testing was used to determine the relative airspeed at which the visual deterrent does not rise from the ground; prior testing at maximum wind tunnel velocity (18 m/s) still demonstrated ~45° relative to ground plane. At the lie-flat velocity (20-25 m/s), turbulence provided dynamic movement, and the flat angle may assist with visibility of the deterrent to eagles overhead under high wind conditions in the field, when Golden Eagles are still known to fly [18]. Given the nominal cut-off speed for operational wind turbines (~25 m/s), this also indicated that visual deterrents are likely to be kinetic whenever the wind turbine is operational.

In Fig. 6b, initial testing of material compatibility of low-cost commercial visual deterrents for long-term use at a wind energy installation is shown. An accelerated weathering testing (AWT) chamber was used to subject visual deterrent textiles to harsh conditions (variable ultraviolet radiation, humidity, temperature, and water spray for approximately 300 hours). The textiles included ripstop nylon (comprising the majority of the deterrent) and a rubberized canvas material (forming the mounting surface to the blower). Two water resistant materials were chosen to use as a comparison: standard truck tarp and a waterproof-breathable clothing textile. Although the textiles showed some loss of coloration, it was similar across samples, and more significant structural degradation was not observed.

Visual deterrent field testing

Visual deterrent field testing involved the deployment of visual deterrent in the presence of wild eagles. This was conducted over two separate field tests in 2018 and 2020 under US Fish and Wildlife Service Eagle Scientific Collecting Permit (MB53604C-0) and Oregon Department of Fish and Wildlife Scientific Taking Permit (010-19, 007-20).

Deterrent Field Test, January 2018:

Siting: The first field test spanned January 25-28, 2018. The selected site was a clearing in the Bear Valley National Wildlife Refuge, located near Worden, OR. Site selection was based on reported high eagle activity, ease of equipment setup, and wide field of view (FOV) for spotting eagles. The site was selected after consulting the U.S. Fish and Wildlife Service (USFWS). The test site was a meadow with relatively dense forestation surrounding the perimeter, near an elevated ridgeline. The visual deterrent (VD) was activated from a hunting blind located approximately 30 meters into the meadow from a fire access road used to access the site.

Data Collection: Two researchers were involved in this field testing. One was dedicated to filming the eagle reactions using a digital camera (DSLR) and directing VD deployment, while the other operated the deterrent and a secondary 360° camera from the hunting blind. Both bald eagles and golden eagles were observed. In all, there were 27 separate eagle sightings across the three days of field testing. Nine videos were recorded during the deployment of the VD. An additional nine videos capture eagle flights without



Figure 6. Left: a close flyby captured during testing. Right: Test setup, with hunting blind and researcher in distance.

the deployment of the VD, for a total of eighteen videos. In instances where eagles were not recorded with the DSLR camera, there may have been multiple birds in the air at once, or the eagle flew over rapidly and could not be captured in time.

Discussion of Results: Of the nine VD videos, four seem to show eagle reaction in the presence of the VD activation. The remainder have difficulty to spot targets, or the target became occluded by clouds or trees before the VD was deployed. In general, eagles tended to stay over the ridgeline, as in **Fig. 7**, which meant that their distance was anywhere from 300-500 meters from the VD and filming location. For most of the videos, the eagles are transiting towards the nearby valley to the east. In some circumstances, the eagles exhibited circling behavior near the ridgeline.

In the most likely example of a potential eagle reaction to the VD, the eagle can be seen circling near the ridgeline; just around the time of deployment, the subject appears to switch to a linear flight path in the direction of the valley. At approximately 30 seconds after deployment, the subject performed one more circling maneuver between 300 and 500 meters out from the VD, then disappeared over the ridgeline and out of line of site (LOS).

While these results may show potential for the use of these deterrents for discouraging activity near wind turbines, insufficient data was collected to provide a statistically relevant conclusion about the effectiveness of the deterrent.

Deterrent Field Test, January-February 2020:

Overview: As before, an outdoor field test was planned to be completed in the vicinity of wild eagles to determine the effectiveness of the system in deterring or altering the flight path of a nearby eagle. The deterrent system consists of kinetic visual deterrent (VD) that can be remotely triggered by a computer using a wireless link. For the planned tests, the deterrent was to be installed in a location of high eagle traffic, and field researchers located nearby would monitor eagle flights and remotely deploy the visual deterrent while recording video footage for analysis of flight patterns. In real time or through post processing, the videos and corresponding field notes could be used to assess if an eagle's flight path had been altered by the visual deterrent deployment. To improve likelihood of useful test outcomes, the field tests were planned in coordination with wildlife biologists, one of whom was present for eagle videography and flight assessment.

Siting: The second field test spanned January 28 – February 3, 2020. The test location and test timing were identified in coordination with U.S. Fish and Wildlife Service personnel, as well as field biologists local to the Pacific Northwest. A test site was identified at a BLM site north of McFall Reservoir, near Klamath

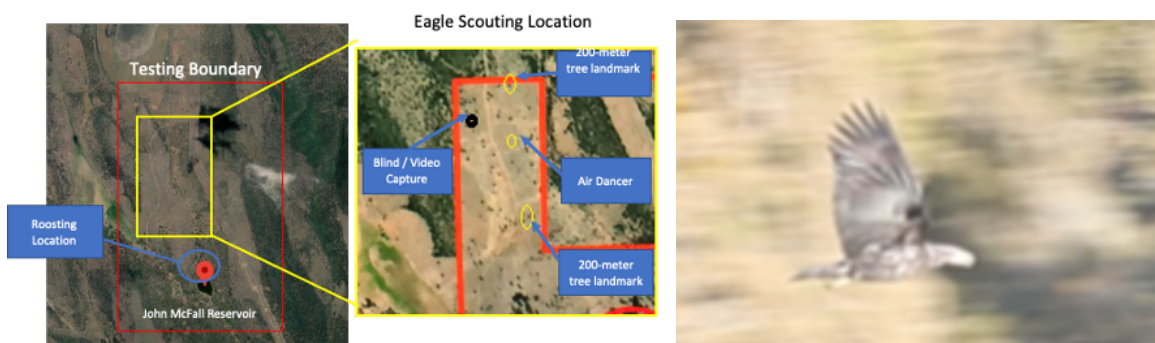


Figure 7. Left: Siting and test setup near Klamath Falls, OR. Right: Frame from video recording using a DSLR with a 600mm zoom lens from the hunting blind.

Falls, OR, where wild eagles roost annually. Many eagles were observed flying over this area during preliminary scouting, and it could be seen easily from various flight paths to the identified roosting area.

The VD was placed in an open field approximately 200 ft east of the area access road. A hunting blind was setup approximately 150 ft west of the road, and all vehicles and non-essential equipment much further north. The visual deterrent system and equipment used for the experiment were setup and disassembled at the beginning of each field test day. As such, the location of the deterrent system and hunting blind changed slightly every day, but by less than approximately 10-20 ft. Two colors and heights of the air dancer were used for this experiment: blue (10 ft) and yellow (30 ft).

Data Collection: Two researchers were involved in this field testing. A wildlife field biologist and wildlife videographer filmed eagle flights and noted observed reactions in real time, while the other operated the deterrent from the hunting blind. Both researchers were located in the hunting blind. Both bald eagles and golden eagles were observed. The two key time frames to obtain wild eagle reaction to the visual deterrent (VD) system would be when they leave the roost to feed after sunrise and when they come back to roost before sunset. When an eagle was spotted flying in the direction of the VD system, the VD was actuated, and eagle behavior was observed and noted in real time, in addition to capturing video through a telescopic lens and DSLR camera. For each recording, the relative elevation of the bird from the VD system was estimated and noted. The VD system was deployed when the wild eagle was approximately 200-300m from the VD; the deterrent was not deployed if the eagle was further away. Written observations were also collected if video recordings were unable to be captured.

Over five observation days, 43 eagles in total were observed, including both golden eagles and bald eagles. Of these, 16 eagle flights were recorded on video; 7 in which the VD was deployed, and 9 in which the VD was not deployed.

Discussion of Results:

For the first field test, eagle reactions were classified using qualitative assessment of change of flight pattern by the field researchers. In the second field test, a similar qualitative metric was used, but in this case assessments were made in real-time by an experienced wildlife biologist, raptor spotter, and wildlife photographer (Bryce Robinson). A majority of the videos and observations noted by the wildlife biologist during the field test demonstrate no clear reaction of observed wild eagles to the activation of the visual deterrent system. Some videos and observations may demonstrate minor reactions but cannot be definitively classified as such. From field notes, one strong observed reaction not captured on video was of an adult bald eagle flying. What is believed to be the same eagle flew approximately 50 ft above the ground during three consecutive days. On the first two days, the yellow visual deterrent was actuated during this bird's flight route with no verifiable reaction. On the third day, the blue visual deterrent was deployed when the

eagle was about 100 m in front of the air dancer, at which point the adult bald eagle reacted demonstrably by flapping its wings and changing its flight path.

While these results may show potential for the use of these deterrents for discouraging activity near wind turbines, insufficient data was collected to provide a statistically relevant conclusion about the effectiveness of the deterrent. Further, over the course of two field test excursion and a total of eight observation days with the assistance of an experience wildlife field biologist and videographer, 25 flights were captured on video, demonstrating the likely challenge in collecting sufficient evidence of deterrent efficacy using this approach.

2.3. Blade Collision Detection System with On-Blade Image Capture (Task 3.00)

Overview and Background

An on-blade, multi-sensor electronic system was developed to monitor blade movement, position, and vibration to detect when an object strikes a turbine blade. A small CMOS imager, similar to a smart phone camera, is integrated in the sensor unit looks down the length of the blade to record video, and a set of image frames can be recorded just before and after a collision or blade strike.

If an impact is detected, images are saved and can be uploaded for off-site analysis of the object striking the turbine blade to enable event confirmation, eliminate false-positives, and allow post-impact species or object identification. Including this combined functionality in the integrated impact minimization system closes a critical loop in validating the efficacy of deterrence, as well as providing ongoing monitoring of impacts and take.

This section summarizes the design and implementation of the on-blade impact detection module (Fig. 8).

On-blade impact detection system architecture

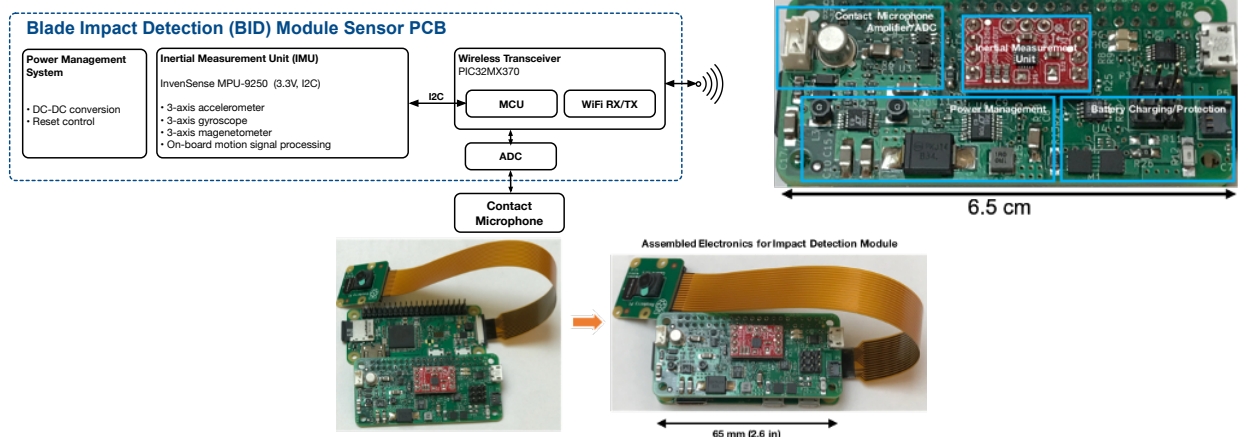


Figure 9. (top) Custom multi-sensor module printed circuit board (PCB) integrates accelerometer, gyrometer, contact microphone readout, and power management into a small circuit board for integration into on-blade system. (bottom) Custom sensor PCB connects to small single-board computer and CMOS imager for complete, wireless system.

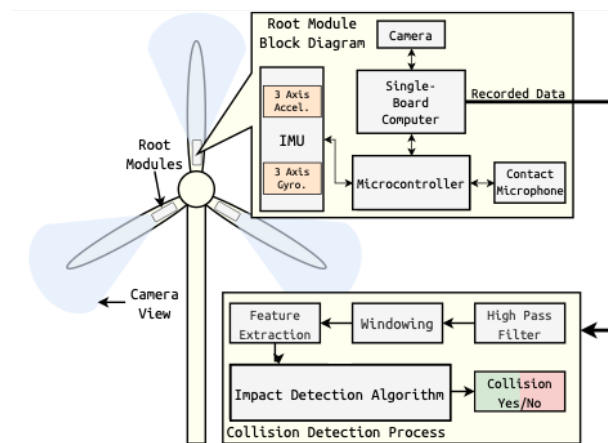


Figure 8. High-level block diagram of on-blade collision detection system with automated image capture of colliding objects.

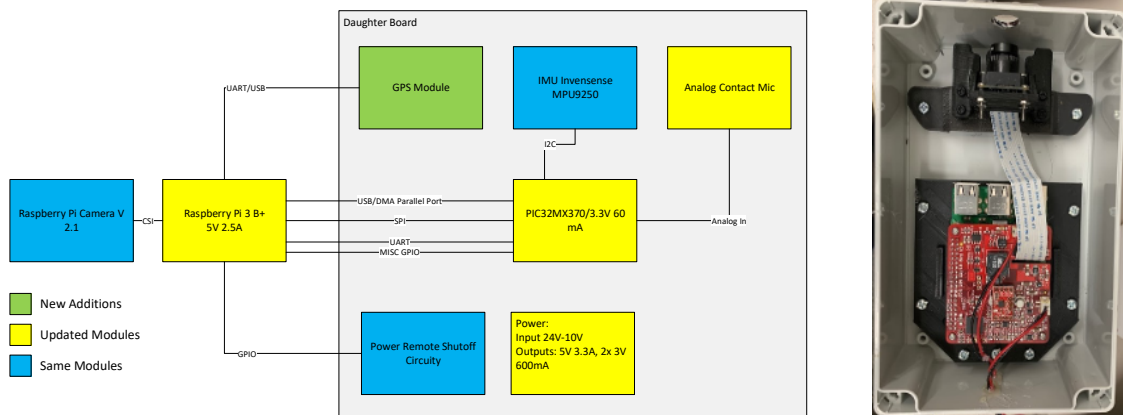


Figure 10. (left) Annotated block diagram of second and final version of collision detection system electronics module following first round of on-blade testing to increase local compute power and improve sample synchronization for IMU and contact microphone data streams. (right) Final system in mounted in custom modified enclosure.

As illustrated in **Fig. 8**, the multi-sensor architecture includes an inertial measurement unit (IMU) that incorporates both accelerometer and gyrometer sensors to measure turbine blade movement and position, a contact microphone for sensing vibration in the turbine blade surface, a small camera for capturing video along the blade length, local on-board computation, and a wireless data connection.

The IMU provides advanced multi-axis motion tracking using an advanced MEMS device. For the blade impact detection (BID) system, the InvenSense MPU-9250 has been selected for its unique combination of low-power consumption in active and idle modes and on-board motion co-processor. From a system level, this IMU will provide: 3-axis accelerometer data, which will provide primary vibration measurement for detecting blade impacts, as well as baseline vibration measurement for correcting for noise in active turbine; 3-axis gyroscope, which can provide blade position and rotational speed at the time of impact; and, a 3-axis magnetometer, which may be used as a compass to estimate turbine position (direction). The IMU accelerometer can operate at up to 4 kHz sample rate, for measurement of up to 2 kHz mechanical vibration frequency, although in most experiments this is operating at a lower 30 Hz sample rate. The IMU requires $<20\mu\text{A}$ under continuous accelerometer operation at 30 samples/second, and $\sim 8\mu\text{A}$ when not in use.

The IMU, contact microphone front-end amplifier readout circuitry, and power management circuitry are incorporated on a custom printed circuit board (PCB), as illustrated in **Fig. 9**. This PCB was designed for direct interfacing with a single board computer (SBC, Raspberry Pi Zero W) and a CMOS image module (Raspberry Pi Camera v.2). The SBC provides system control, data logging, video capture, and wireless data interface over 2.4GHz WiFi. The integrated sensor system shown in **Fig. 9** was used in initial on-blade testing (Section 4.00). Following initial testing, an enhanced BID electronic subsystem was developed, shown in **Fig. 10**, which adds a secondary microcontroller (PIC32MX) for time synchronization of the IMU and contract microphone data streams, and uses a more powerful SBC (Raspberry Pi 3B+) to provide additional local computer power for automated collision detection algorithms.

Custom firmware for the microcontroller was developed in C, which configures all system sensors and streams time-synchronized digital data from the IMU and contract microphone to the SBC. Custom software for the SBC was developed for recording sensor data, looping and recording on-blade camera data, and providing wireless control and data access was developed primarily in Python.

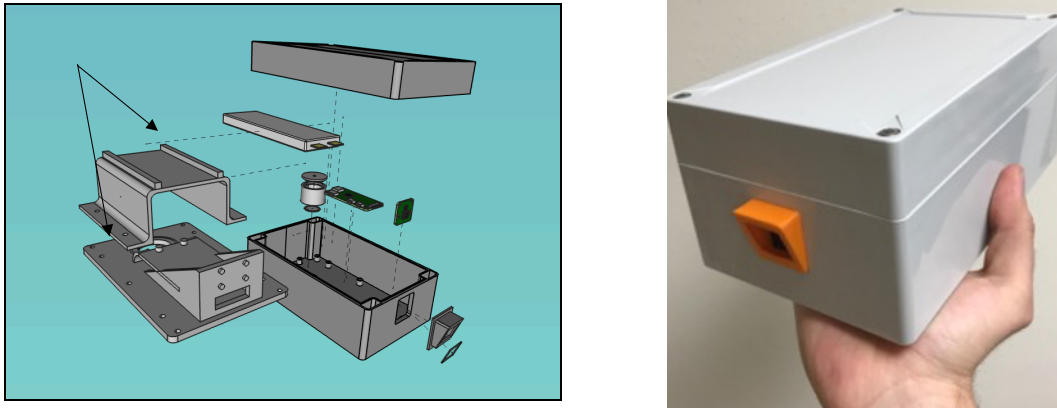


Figure 11. (left) Exploded view of the mechanical housing for BID system and corresponding electrical components. (right) External view of assembled BID module in modified IP67-rated enclosure.

Blade impact detection system enclosure and fixturing

A mechanical housing for the BID was designed for containment and protection of all electrical components while installed for on-blade testing on an operational wind turbine, which is detailed in **Fig. 11**. The enclosure is a modified IP67-rated commercial enclosure. Custom internal fixtures include two additively manufactured pieces to mount the SBC, camera, multi-sensor PCB, and other component.

Blade impact detection system laboratory testing

Laboratory-based testing and verification of the BID module electronics was conducted using a test stand, which was constructed to apply repeatable impacts both with and without added system noise for verifying functionality of hardware, firmware, and software, and for initial development and validation of automated collision detection algorithms. As pictured in **Fig. 12**, the test stand includes a beam anchored at one end as a test object, a collision detection module with CMOS image sensor installed at the anchored root of the beam, and an automated dropper installed above the beam tip.

A mechanical shaker is attached to the free end of the pipe. The shaker is setup to add mechanical vibrations onto the pipe to test the system's ability to handle noise, simulating the mechanical noise induced on a turbine blade. The shaker is set to vibrate the pipe with a waveform superimposing a 20Hz sine wave and a gaussian white noise source. To test the impact detection the system was tested with no noise (idle), and using an input noise level of 10 mV RMS, 15mV RMS, and 20 mV RMS.

The impact detection module captures a video sample when triggered by the automated detection of an impact (Section 3.4), in order to capture still frames before, after, and at the point of impact. As tested, the CMOS image sensor runs a continuous loop buffer, and each automatically captured video file is a 10 second clip of the impact with video centered on the impact (showing 5 seconds before and after the impact detection).

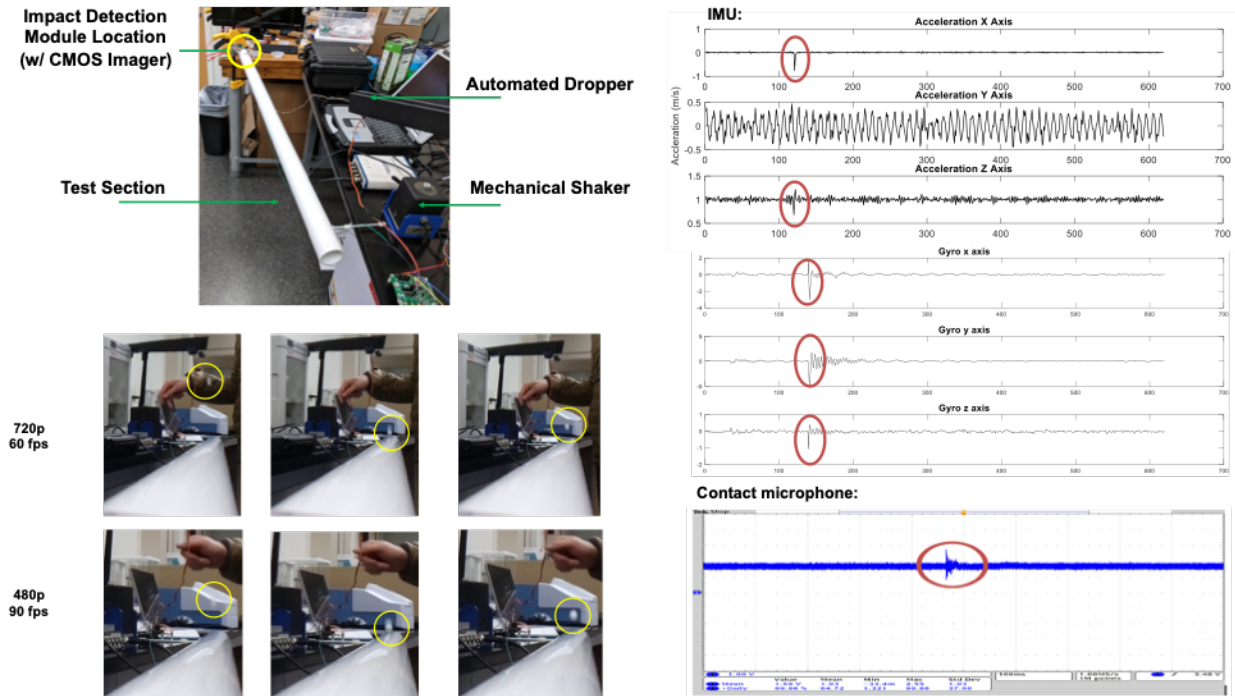


Figure 12. (left) A test apparatus constructed to verify functionality of collision detection and image capture subsystems, including automatically captured image frames from a detection collision. (right) Raw sensor data gathered from the accelerometer and gyrometer on the system, as well as from the contact microphone interface. Sample test impacts are annotated and appear across all channels. Data shown was recorded in the presence of induced mechanical vibrations from the shaker, which is most visible in the y-axis accelerometer recording.

Typical test data are shown in **Fig. 12**, where raw sensor data recorded by the BID electronics include 3-axis accelerometer and 3-axis gyrometer from the IMU, as well as digitized contact microphone data. A preliminary threshold-based impact detection algorithm was used for collision detection, which automatically stores to memory the most recent video buffer, providing image capture of the colliding object. In addition, both Bluetooth and WiFi wireless connections to the integrated BID electronics were tested to verify system connectivity for overall system integration.

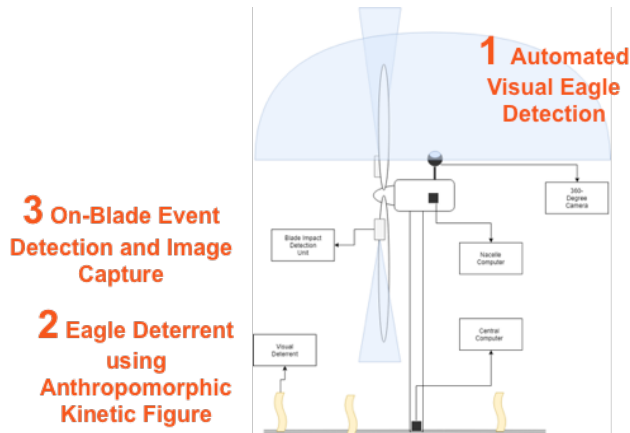
2.4. System Integration and Full System Testing (Task 4.00)

Overview and Background

Full-system field testing was conducted in an outdoor field environment on the Corvallis campus of Oregon State University to verify all system functionality following relocation from the indoor laboratory environment to a separate outdoor location, including transport and assembly of all system components. This complete test served as a ‘dry run’ in advance of follow-on testing on full-scale wind turbines at Mesalands Community College and NREL-NWTC.

Overview of eagle detection, collision detection, and eagle deterrent integrated system:

- 360° camera mounted on nacelle
- On-blade collision detection on each blade (3X)
- Kintetic visual deterrents with remote trigger
- Computation and control in nacelle and on ground



Data and control integration map:

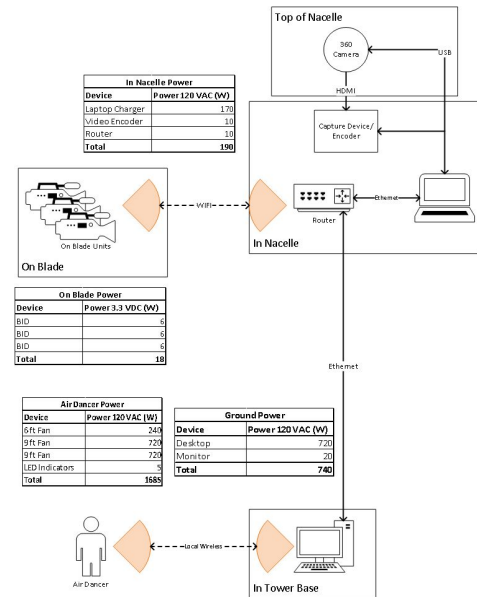


Figure 13. (left) Intended location of detection, deterrent, and collision detection system components on an installed wind turbine. (right) Network diagram including wired and wireless connections among subsystems for control and data acquisition across the integrated system.

System integration

The overall system architecture is illustrated in **Fig. 13**, where a combination of wired and wireless connections is used for system integration, control, and remote data acquisition. Each on-blade collision detection and image capture module connects to a router in the nacelle through a 2.4GHz WiFi link. The 360° camera is installed atop the nacelle and is connected over wired USB and HDMI connections to a video encoder and computer located in the nacelle; this computer provides local video stream processing for broadcast to the turbine base, and it provides wireless control and data interfaces for on-blade modules.

A wired ethernet or fiber optic link connects the nacelle computer to a central computer located in the tower base; this central computer provides additional computational processing power for operation of real-time video stream processing and eagle detection algorithms.

Visual deterrents are triggered remotely, and both wired (RS-485) and wireless (sub-GHz) links were developed and tested. Custom software handlers running on the nacelle and tower base computers were used for remote control of and data acquisition from on-blade modules, as well as providing manual and automated triggering of visual deterrents.

In addition to the development of a connection network and handling software, additional custom fixturing was designed and fabricated for mounting the 360° camera on the nacelle, and for providing power to on-blade modules through the turbine hub slip ring; these are shown in **Fig. 14**.

Summary of full-system field tests:

Following benchtop validation of individual and integrated system components, the complete system was disassembled in the lab and relocated to a combined outdoor/indoor field test location on the Oregon State University campus. Subsystems intended for outdoor use, including visual deterrents, impact detection modules, and 360° eagle detection camera, were located outdoors to mimic real environmental operating conditions; subsystems intended for indoor use, include the tower base computer (algorithm processing) and in-nacelle computer (wireless interface to and control of blade-mounted modules and nacelle-mounted



Figure 14. (left) Additional custom fixturing was designed and fabricated for mounting 360° camera on the nacelle. (right) Custom DC-DC power conversion assembly for powering on-blade modules from the turbine hub.

360° camera) were set up at an adjacent indoor location to mimic operational conditions. Testing proceeded over the course of a day; all tests were tested multiple times (generally three) for robust verification, and all were successful.

Blade Impact Detection (BID) Sub-system: Successful verification of the blade impact detection module included: on/off control by the tower computer, simultaneous wireless connection to all three impact detection modules, on-blade camera communication and alignment, on-blade camera exposure calibration and image capture, recording of raw data files from all on-blade sensors (contact microphone, accelerometer, gyrometer), simultaneous continuous recording of on-blade videos and sensor data streams (static, moving, and tapping), and deterrent trigger recording using artificial stimulus.

Visual Deterrent Sub-system: Successful verification of the visual deterrent detection module included: basic on/off control of visual deterrent fan module, remote on/off control using a wired connection, remote on/off control using a wireless link, remote visual deterrent start-up in random sequence following a software-define signal, and automated remote triggering of visual deterrent start-up using an artificial stimulus representing ‘eagle-detected’ signal.

Wireless Connectivity Testing: Successful verification of the wireless system connections included: communication range testing between the tower computer and the remote visual deterrent control box with verified range exceeding 250 meters, and verification of the communication range between the BID on-blade units and the in-nacelle computer exceeding 10m. All wireless connections were verified for connection, data transfer for control, and re-connection after power cycling.

360° Camera Sub-system: Successful verification of the 360° camera sub-system for on-nacelle use included: on/off control and start/stop recording by via wireless network connection verification of recorded file name and location, video recording and real-time streaming over the wired network, and verification of video recording exposure control in multiple lighting conditions. Additional field testing of the automated eagle detection hardware and software sub-system in the presence of live birds was conducted in an outdoor field environment at the High Desert Museum in Bend, OR to verify all system functionality following relocation from the indoor laboratory environment to a separate outdoor location, including transport and assembly of all system components, and including classification of live birds (eagle and non-eagle). These field tests were further detailed in Section 2.1.

Through these tests, all sub-system functionality and interconnectivity was successfully validated.

3. Summary of Field Testing (Task 5.00)

Three separate field tests were conducted over the course of the project to validate functionality of the complete integrated detection and deterrent system on an operational wind turbine, and to provide real-world data on which to develop, train, and test automated impact detection algorithms. This section summarizes each of these field tests, including installation, data collection, and lessons learned for future development.

3.1. Field Testing at NREL-NWTC, Boulder, CO – October 2018

Field Test Overview

The first round of on-turbine field testing was completed 10/15/18-10/19/18 on a 1.5MW GE wind turbine at the NREL National Wind Technology Center (NWTC) facility, located at the Flatirons Campus in Boulder, CO. The primary intent of these field tests was to verify installation and operation of the complete integrated detection and deterrent system using an operational wind turbine, and to provide initial sensor data recording from all sensors and cameras, both for downstream analysis and to be used for further system improvement in advance of additional on-turbine testing in future field tests. For eagle detection, programmed fixed-wing drone flights were used as surrogate birds for evaluation of the 360° imaging system. For blade strike and collision detection, small surrogate projectiles were used. In addition, data was recorded from all sensors across multiple operational conditions for downstream assessment. Test planning, coordination, and execution was done in close collaboration with NREL-NWTC staff.

Installation of blade impact detection (BID) modules and 360° camera

BID modules were installed onto the root of the leading edge of each of the three turbine blades, as shown in **Fig. 15**. Each unit was secured to the blade surface using 3M VHB double sided tape following surface cleaning. Each module was positioned with the on-blade camera facing down the leading edge of the blade. As an additional measure, the bottom perimeter of the box was secured with additional tape, and a tape strap was applied across the box and secured to the blade.



Figure 15. Installation of multi-sensor modules and contact microphones on each blade of a GE 1.5MW wind turbine for collision detection and image capture, and a 360° camera installed on the nacelle roof for eagle detection.

A contact microphone was installed on the blade next to each BID module using tape. Care was taken to ensure that the entire metal surface of the transducer was in contact with the blade's surface.

The BID units were powered using a Sola power supply connected to a service power outlet in the hub of the turbine. The power wires were run through the hub shroud to each blade unit. Cables were connected to the units via a service loop for strain relief, and excess wire was secured to keep it free of any moving parts during blade pitching.

The 360° camera was attached to the nacelle mount by telescopic monopod and C-clamps, as shown in **Fig. 16**. The nacelle mount connected to an existing lidar bracket on the nacelle roof and was secured by an aluminum adapter with angle bracket through hole. Power and data cables for the camera routed through an access hatch in the nacelle and connected to the nacelle computer for video data stream processing.

As illustrated in **Fig. 13**, a wireless router and compact computer were installed in the nacelle for wireless connection to all three on-blade modules and wired connection to the 360° camera, and a separate computer was installed in the tower base for real-time video stream processing.

Installation and test of visual deterrent system

The visual deterrent system was installed on ground, with an approximately 10 meters distance next to the turbine tower base, as shown in **Fig. 16**. The visual deterrent controller ('Remote System Box') communicates with the tower base computer through a local sub-GHz wireless link. As the eagle detection algorithm runs on the tower base computer, this enables automated deterrent triggering based on a programmable threshold of eagle classification confidence.

In our field testing, we successfully triggered the visual deterrent by remotely sending trigger signals representing artificial stimuli; in practice, this would be triggered by the eagle detection system if eagles were detected in the 360° camera video stream from the nacelle roof. As tested, the communication range between the tower computer and the visual deterrent control box can be greater than 250 meters.



Figure 16. Installation and testing of visual deterrent near the base of the 1.5MW wind turbine. The deterrent is activated by an artificial stimulus; in practice, this would be triggered by the eagle detection system (Task 1.00) if eagles were detected in the 360° camera video stream from the nacelle roof.

Data collection from 360° camera using drone flights

Video streams from the 360° camera to the in-nacelle laptop via HDMI, and an example 360° video frame is shown in **Fig. 17**. As can be noted it provides a field of view of the entire azimuthal sweep (North, South, East West) and the elevations expected for the species of interest (e.g. eagles).

A fixed-wing drone was used as an eagle surrogate, providing images of a known-size flying object from various 3D positions relative to the 360° camera. Direct triggering of visual deterrent from drone was not possible, as the classifier is trained for eagle/non-eagle and not for drones (all non-eagle); as such, this was not a test of the binary eagle classifier. Instead, drones were used to capture relevant video from the nacelle with an object of known size and known (via GPA) distance from the camera. A total of five drone flights were performed near the wind turbine, following installation and initial validation of the 360° camera system. The operating drone, a FireFLY6 PRO, has a wingspan of 1524 mm and length of 828 mm with a cruise speed of 30-35kts (15-18m/s), as shown in **Fig. 17**; this is comparable to a typical eagle soaring speed of ~14-15 m/s. Drone flight paths were recorded using on-board GPS; for the path shown in **Fig. 17**, the maximum distance from the camera position to the drone is approximately 350 meters. Flight paths included loops up to 600m from the turbine tower.

An example drone image is shown in **Fig. 18**, where the drone is approximately 75m from the turbine tower. The green bounding box was generated by an automated motion detection algorithm running in real-time to mimic the eagle detection algorithm; this is approximately 40 x 40 pixels. The minimum drone image detected by the motion detection algorithm is 10 x 10 pixels, and the minimum drone image recognized by visual inspection is 5 x 5 pixels. As the 360° camera's hemispherical lens indicates pixel density decreases approaching the zenith (i.e. center of the image), objects that are nearer or below the horizon will have a higher pixel density for the same distance from the camera. While an important performance tradeoff for single-imager 360° cameras, in this application it is possible (though not tested here) that the higher pixel density at the horizon may be beneficial for longer-range detection.

Data collection from on-blade modules

Figure 17. Sample image from nacelle-mounted 360° 4K camera (left); fixed-wing drone used for programmed flights and 360° capture (middle); and, GPS recording of drone flight relative to the wind turbine and camera position (right).

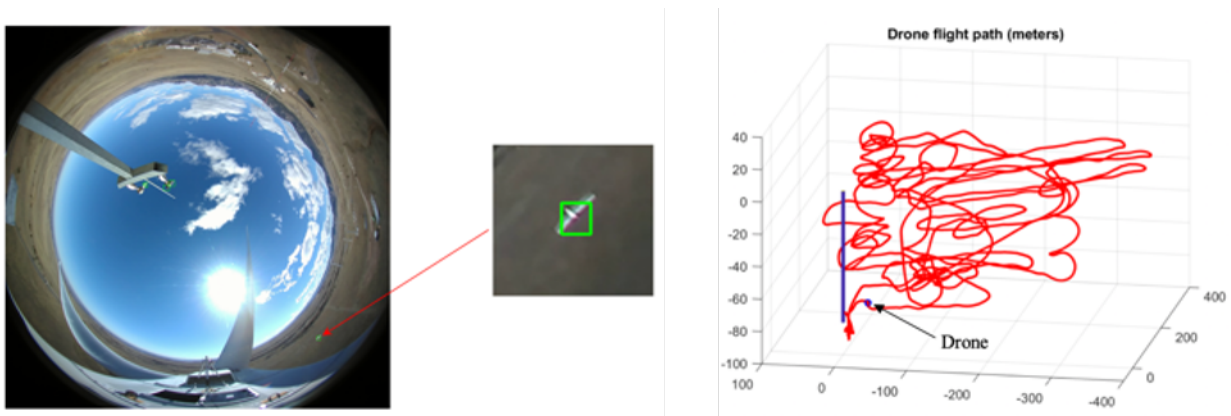


Figure 18. Sample image from nacelle-mounted 360° 4K camera (left); zoom in of fixed-wing drone in 360° camera frame with automatic bounding box based on motion detection (middle); and, GPS recording of drone flight relative to the wind turbine and camera position (right).

Following installation of on-blade collision detection modules, a series of tests were performed to verify that the units were operational. After power-on, the BID modules automatically connected to the local wireless network, and all additional tests were performed over remote log-in to the BID modules through the wireless network.

Each sensor was verified, as shown in **Fig. 19**. A still image was taken from each on-blade imager to verify that the camera was aligned and in focus. Simple tapping tests were performed with a rubber mallet to verify contact microphone functionality, and for downstream analysis of sensitivity to detecting vibrations. Tapping locations included each blade next to the installed BID module, on the shroud of the hub, on the upper tower wall, and on the base of the tower.

A variety of turbine motions were performed while recording from all contact microphone and IMU sensors: single blade pitching for each blade, all blades pitching simultaneously, turbine in normal running mode, turbine while generating power, turbine stopping, and on a stopped turbine. As an example, **Fig. 19** shows recorded accelerometer data from a blade pitching from 85° to 0°.

Over the course of the field test, a total of 25 tapping and turbine motion experiments were recorded, resulting in multi-sensor data recording across all three blades.

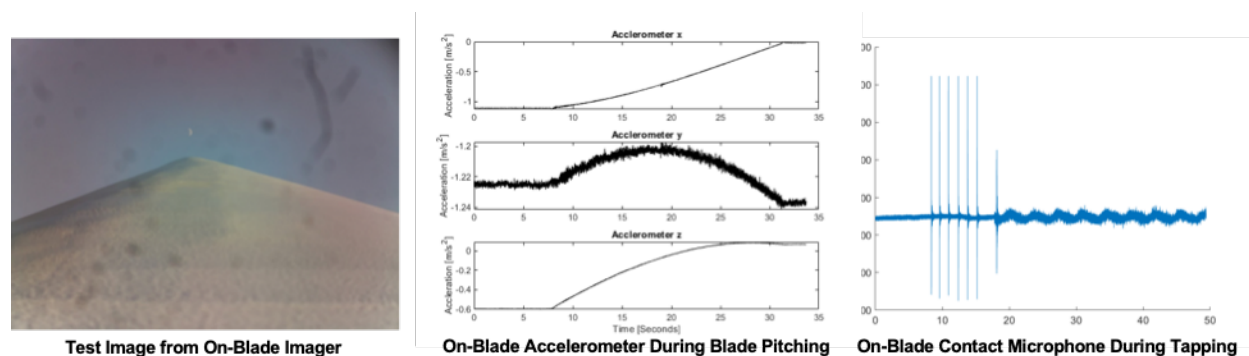


Figure 19. Initial validation of on-blade collision detection modules includes remote testing of all sensor subsystems; on-blade imager for down-blade image capture, on-blade IMU (accelerometer and gyrometer), and on-blade contact microphone. All three on-blade modules were validated following installation prior to structured data collection.



Figure 20. Surrogate blade strikes were conducted using soft projectiles fired at the blade using compressed air. Shown at right is an image of two tennis balls just after striking the blade, captured automatically by the on-blade collision detection module.

Surrogate blade collision tests

To emulate avian blade strikes, surrogate projectiles were launched at the turbine under a variety of operation conditions, while on-blade collision detection modules recorded signals on all three blades. Projectiles included normal tennis balls, tennis balls filled with water, and small fingerling potatoes, fired using compressed air. A boom lift was used to fire from a position closer to the turbine blade, approximately 100ft from the ground. These tests include: shooting at a still turbine with normal tennis balls, shooting at a moving turbine with normal tennis balls, moving turbine with filled tennis balls, and moving turbine with potatoes.

In summary, we successfully recorded 14 impact events for regular tennis balls interacting with stationary blades, 12 impact events for regular tennis balls interacting with rotating blades, 16 impact events for tennis balls filled with water interacting with rotating blades, and potatoes interacting with moving blades. Field notes were taken on-site for each impact.

An example data recorded during a tennis ball impact is shown in **Fig. 21**, recorded by the on-blade module on the struck blade. The slow oscillation seen in the accelerometer data correspond to the wind turbine blade rotation.

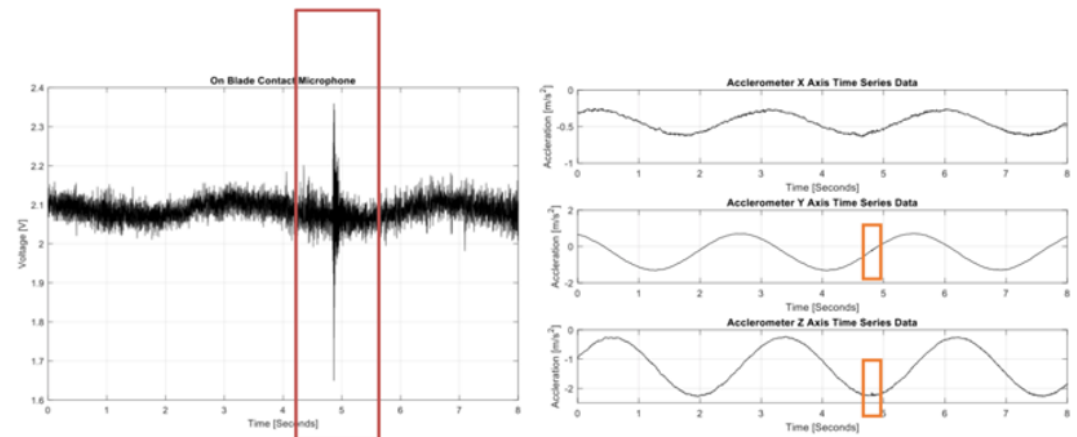


Figure 21. Blade strike by surrogate projectile (tennis ball) recorded using the on-blade sensor module.

Summary of data collected

Over the five-day field test, installation procedures and baseline functionality of all hardware subsystems and real-time communication among all parts were verified, including 360° visual detection from the nacelle, ground-based visual deterrent deployment, and on-blade sensing and imaging for collision detection. The eagle classification algorithm was not included in this testing.

Video recordings of five fixed-wing drone flights were taken from the nacelle-mounted 360° camera, allowing downstream analysis of object size vs. distance and pixel density for the selected camera module. The visual deterrent system was successfully operated on-site with a trigger signal simulating eagle detection. More than 300 separate multi-sensor recordings were created using the on-blade collision detection modules, providing a rich data source for downstream analysis of on-blade baseline vibration and motion artifacts. Multi-blade recordings for more than 40 surrogate projectile impacts can be used for offline development and test of collision detection algorithms using real-world data. Preliminary thresh-hold based detection demonstrated viability of the automated image capture functionality.

3.2. Field Testing at Mesalands Community College, Tucumcari, NM – April 2019

Field Test Overview

The second round of on-turbine field testing was completed 04/29/19-05/03/19 on a 1.5MW GE wind turbine at the North American Wind Research and Training Center (NAWRTC) facility at Mesalands Community College, Tucumcari, NM. Between the previous field testing at NAWRTC and this second field test, the on-blade collision detection module internal electronics were redesigned as described in Section 2.3 and shown in **Fig. 10**, based on lessons learned from the first round of field testing and post-test data analysis. As such, the primary goal of this second on-site field test was verification of subsystem functionality and real-time communication among all parts; updated on-blade impact detection and imaging modules, nacelle-mounted 360° camera, and ground-based visual deterrent system. This verification was successfully achieved. The eagle classification algorithm was not included in this testing.

Vibration data were recorded by accelerometers, gyrometers, and contact microphones integrated in the on-blade units for a variety of operational conditions and turbine motions, including free



Figure 22. Installation and verification of system components on a 1.5MW GE wind turbine at NAWRTC, Mesalands Community College, Tucumcari, NM.

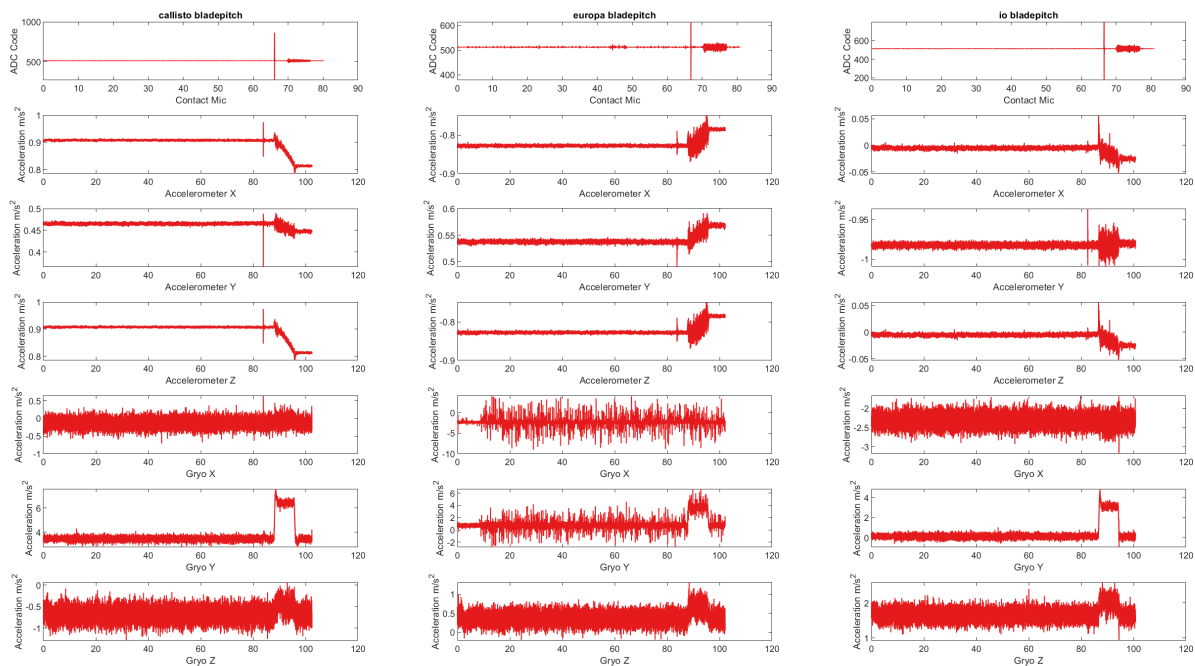


Figure 23. Typical data recorded from on-blade multi-sensor modules, with blades pitching from 85° to 0° ; pitching begins at approximately 85s, and the impulse visible just prior to this is the mechanical pitching lock being opening at the blade hub.

and generating rotations, blade pitching, and nacelle rotations. Down-blade images were successfully captured by the on-blade unit. Test impacts using surrogate objects were performed, providing recorded on-blade vibration data for 15 confirmed impacts. Tapping tests and free-running recordings provide additional information on vibration sensitivity and background noise. The kinetic visual deterrent system was successfully operated on-site, triggered remotely following a signal of a simulated eagle detection.

System Installation

As updates to the collision detection module were largely internal, installation procedures followed the same process as in Section 3.1 and are not duplicated here. An overview of the installed system components is provided in **Fig. 22**.

Data collection from on-blade modules

Data collection proceeded as in Section 3.1, including post-installation system verification and recording across all sensor modules. As before, sensor recordings were taken across multiple turbine movements: blade pitching, turbine yawing, turbine running, turbine braking, turbine shutdown. A typical recording of all blades pitching from 85° to 0° is shown in **Fig. 23**. A total of 11 turbine motion event trials were recording across all three on-blade modules.

Tapping tests were also conducted as in Section 3.1, including tapping locations on each blade and on the turbine tower; a typical recorded tapping test is shown in **Fig. 24**.

Surrogate blade collision tests

Blade collisions were performed using surrogate projectiles following the same procedure described in Section 3.1. However, as at NWTTC there was no access to a boom lift to elevate the air cannon, overall accuracy and efficiency of our impact simulation testing was reduced.

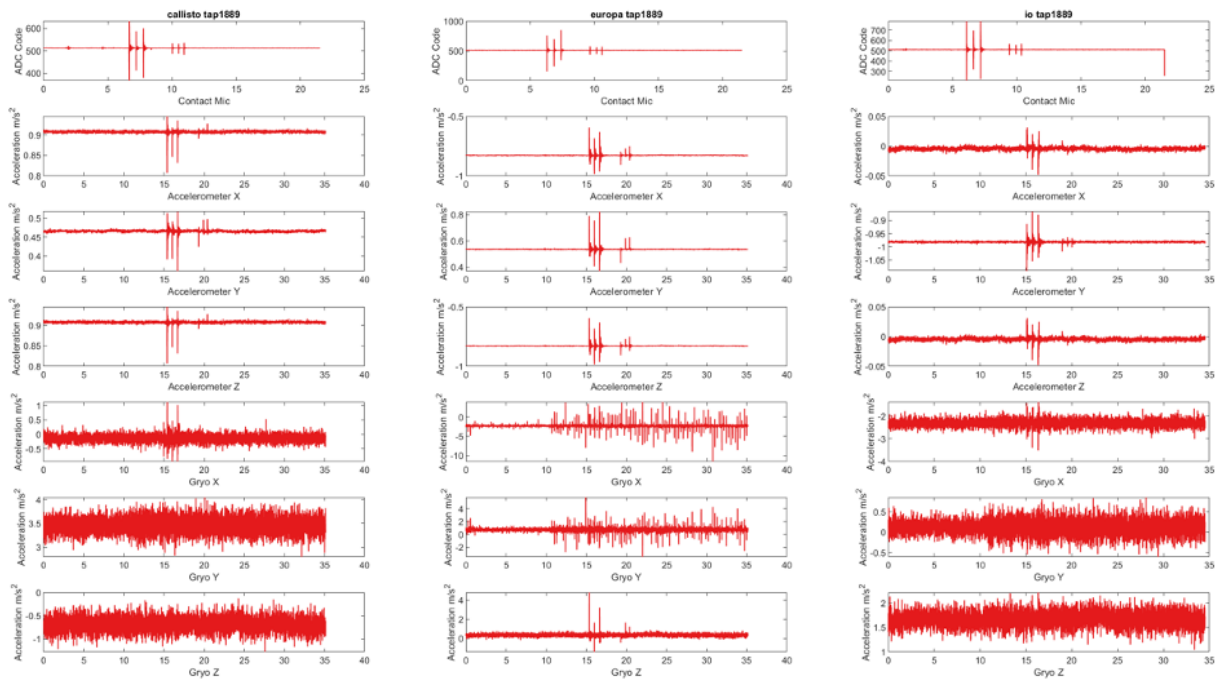


Figure 24. Typical data recorded from tapping on one of the blades (middle column), with the resulting vibrations seen across sensors (accelerometer, contact microphone, gyrometer) and across all blades.

Combined with weather and installation delays, only one field test day was used for blade strike testing, during which we collected 55 recordings (55 on each on-blade module), with 13 of those recordings containing blade impacts.

Summary of findings

A primary goal of this testing was to verify our installation procedures and test methods in preparation for our final round of up-turbine testing at NREL later in 2019. While onsite at Mesalands, we were able to fully install the entire system on the wind turbine, verify correct functionality of all hardware components, and disassemble the system. The eagle classification algorithm was not included in this testing.

The BID modules for these tests used an improved version of the contact microphone recording electronics that were used in our previous NREL-NWTC tests. Analyzing the frequency content of the new contact microphone data, we can see improvement over the prior contact microphone circuit at eliminating the 60 Hz line noise tone and its harmonics.

Fig. 25 highlights the new contact microphone signal in the presence of a surrogate impact event by a tennis ball. In this it should be noted that the average noise level is lower, less than 3 analog-

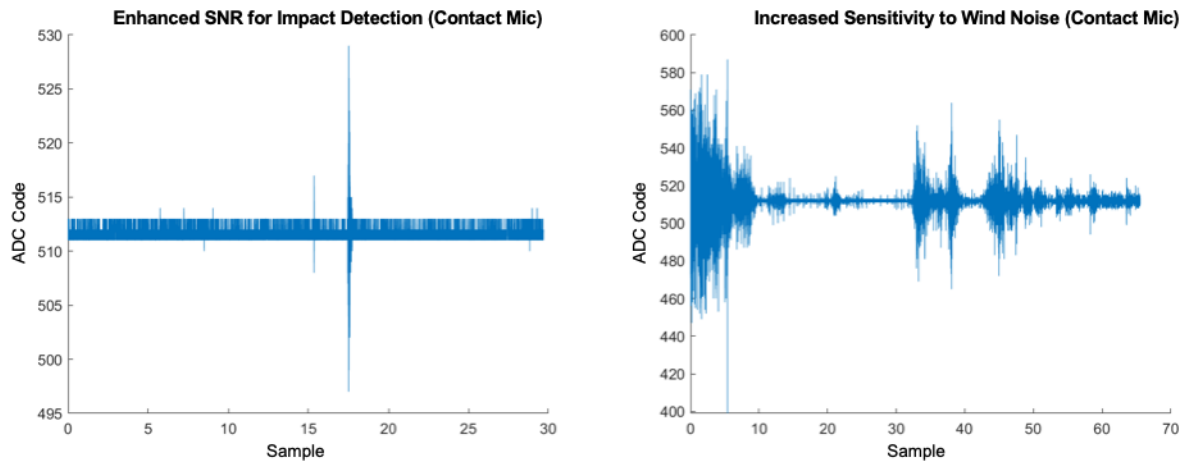


Figure 25. SNR is improved over the prior system (left); increased sensitivity also picks up more wind noise while mounted on the blade, so future installations will include a wind cover (Section 3.3).

to-digital converter (ADC) codes (y-axis), or about 9 mV, and without the low frequency or 60 Hz noise present in the prior contact microphone signals.

Continuing the analysis of the new contact microphone data we find that the new system is more sensitive to vibration and impacts. In designing the updated contact microphone circuit, additional gain was provided to further amplify the signal in hopes to increase sensitivity for collision detection. This had a side effect of causing the system to be more sensitive to wind noise on the contact microphone (**Fig. 25**), which will be mitigated by improved wind isolation in future tests, as described in Section 3.3.

3.3. Field Testing at NREL-NWTC, Boulder, CO – July 2019

Field Test Overview

The third and final round of on-turbine field testing was completed July 19-26, 2019 on a 1.5MW GE wind turbine at the NREL National Wind Technology Center (NWTC) facility, located at the Flatirons Campus in Boulder, CO. All systems were installed and verified for functionality and systems communication. Tests employed the final iteration of the multi-sensor on-blade modules, including enhanced contact microphone electronics and updated mounting approaches, incorporating learnings from the previous NWTC tests. Over several days, data was recorded using multi-sensor modules installed on all three turbine blades, in a variety of operational conditions (rotating, idle, pitching, generating, etc.). The eagle classification algorithm was not included in this testing.

Among planned and verified test objectives, the visual deterrent was tested with automatic deployment after target motion, and multiple unmanned air vehicles (UAV) flights were performed; 360° camera footage was taken of the programmed UAV flights, as well as from an additional (non-360°) nacelle-mounted camera. Numerous artificial blade impacts were performed using tennis balls and organic projectiles in multiple operating conditions and recorded. Test planning, coordination, and execution was done in close collaboration with NREL-NWTC staff.

System installation and data collection

Installation procedures followed the same process as in Section 3.1 and are not duplicated here. The primary modification is the installation of a custom wind cover for the contact microphone at each on-blade collision detection module to decrease baseline noise. An overview of the installed up-turbine system components is provided in **Fig. 26** and **Fig. 27**.

Summary of data collection from integrated system components

Data collection proceeded as in Section 3.1, including post-installation system verification and recording across all sensor modules, as well as surrogate blade strikes using projectiles launched from a boom lift; representative images are shown in **Fig. 28**. As before, sensor recordings were taken across multiple turbine movements: blade pitching, turbine yawing, turbine running, turbine

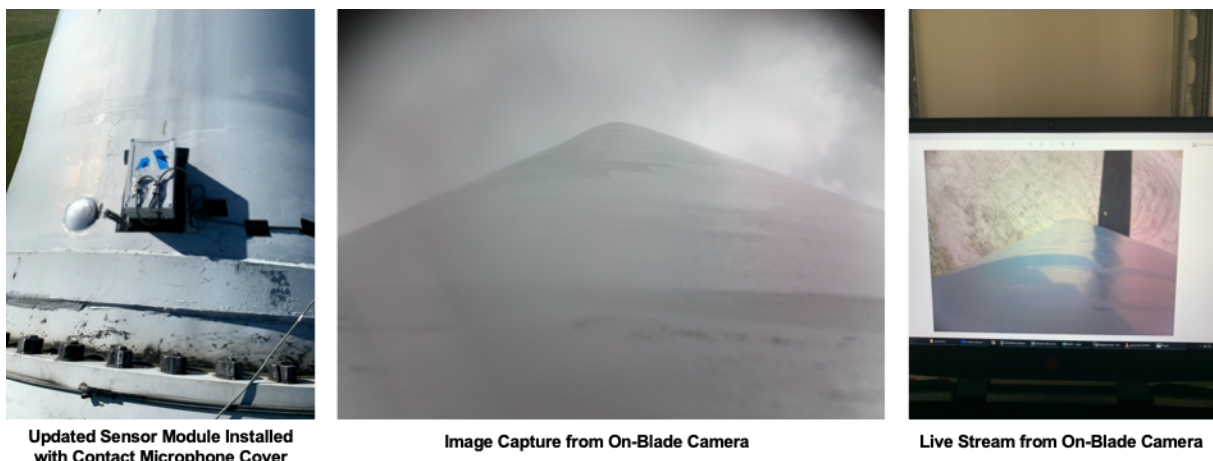


Figure 26. Installation and of final on-bladed system components on a 1.5MW GE wind turbine at NREL-NWTC in Boulder, CO. Multi-sensor module is shown, along with image capture and live stream from on-blade imager. The contact microphone now includes a custom wind cover to mitigate added wind noise sensitivity (Fig. 25).

braking, turbine shutdown. Overall, 214 multi-sensor data recordings were recorded from the blade sensors including 70 surrogate blade strikes, providing a rich data source for algorithm development. Representative on-blade sensor recordings are shown in **Fig. 29-32**, including blade strike images captured automatically by the on-blade imagers following detection collisions.



Figure 27. Installation and of final nacelle system components on a 1.5MW GE wind turbine at NREL-NWTC in Boulder, CO providing both 360° camera and high-resolution camera images and video for testing.



Figure 28. Data collection includes surrogate blade strikes using projectiles (tennis balls and potatoes), as well as programmed fixed-wing UAV flights for recording 360° and high-resolution video images from the nacelle.

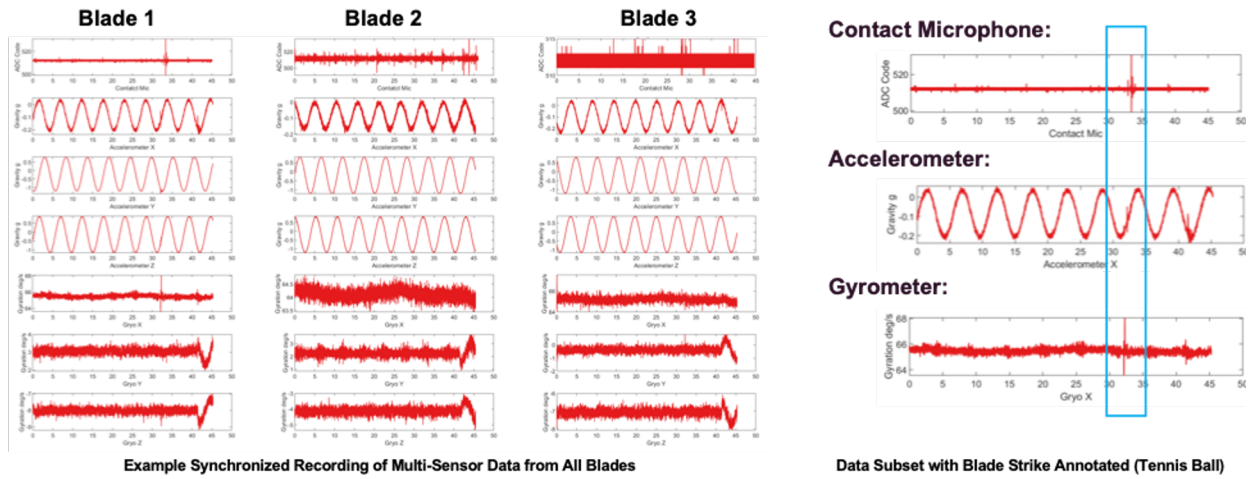


Figure 29. Example time-synchronized data taken across all three blade-mounted sensor modules (left); and, subset of Blade 1 sensor data with a tennis ball impact visible on all sensor types (right).

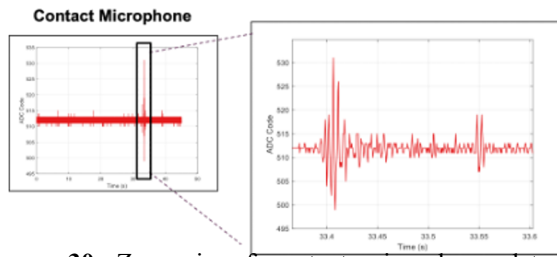


Figure 30. Zoom in of contact microphone data during a blade collision using a tennis ball as a surrogate projectile.

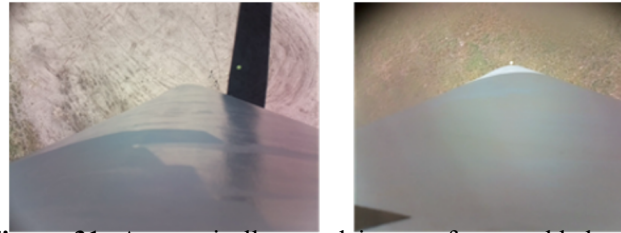


Figure 31. Automatically saved images from on-blade imager following detected collisions; tennis ball is visible in frame, providing record of striking object.

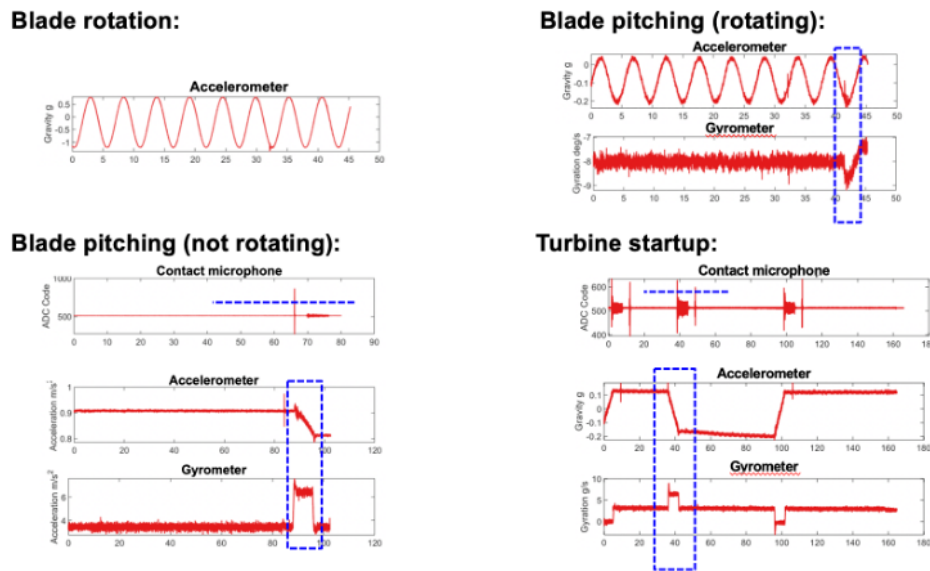


Figure 32. Annotations of typical non-collision turbine and blade actions visible from on-blade sensors, including blade rotation, blade pitching, and turbine startup.

3.4. Development of automated collision detection algorithms

The extensive on-blade sensor recording data set, including more than 200 multi-blade recordings and 70 surrogate blade strikes, was used to develop enhanced automated collision detection algorithms. The approach and findings are summarized here, with additional detail available in [9] and in future publications as algorithm development continues. A high-level illustration of the signal processing and collision detection process is illustrated in **Fig. 33**, including filtering, windowing, standardization, and the use of a trained AdaBoost random forest classifier.

On-turbine sensor data can be divided up into three different turbine operational modes occurring during the testing: stopped, spinning, and idle. A stopped turbine occurs during instances with very low wind velocity, and the turbine blade is not rotating; this can be seen with near-zero slope in the accelerometer data. Spinning occurs when the turbine is spinning at its operational rate of rotation and can be characterized by a steady fixed frequency sine wave signal in the accelerometers. Finally, idle operation occurs with sufficient wind velocity for rotation, but insufficient for rotation at operational frequency. For developing the detection algorithm, analysis was focused on the spinning mode data sets, which present the greatest threat for avian collisions.

Visual analysis of the signals gathered highlight the main challenge in automatically detecting colliding objects on the wind turbine (**Fig. 33**). While known collisions stand out, it is difficult to define a level where a spike is due to an object hitting the wind turbine blade, or due to other turbine-related events such as blade pitching or nacelle yaw. Analysis from [10] shows signals overlapping in the frequency spectrum and notes the difficulty of a threshold-based detection algorithm. To overcome these challenges, we have employed an AdaBoosted random forest ensemble for collision detection [11]–[13].

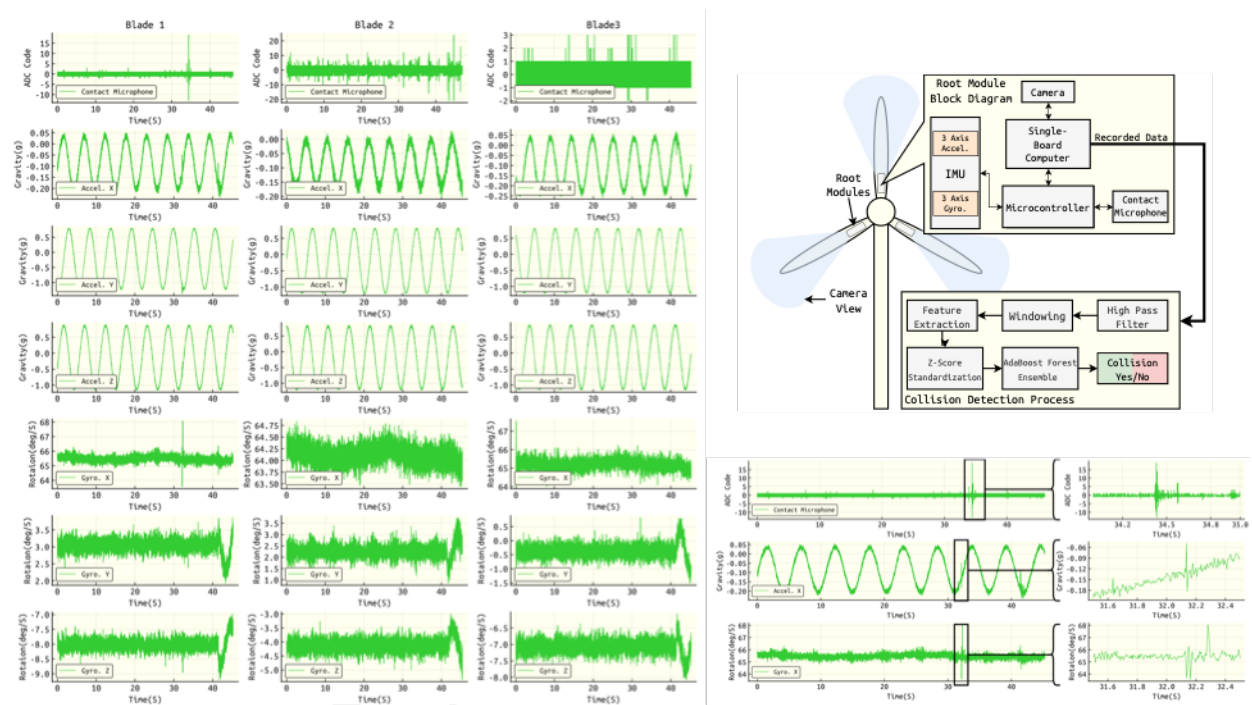


Figure 33. Three-blade multi-sensor data (accelerometer, gyrometer, contact microphone) is used as input to train a collision detection classifier algorithm for automated blade-strike collision detection.

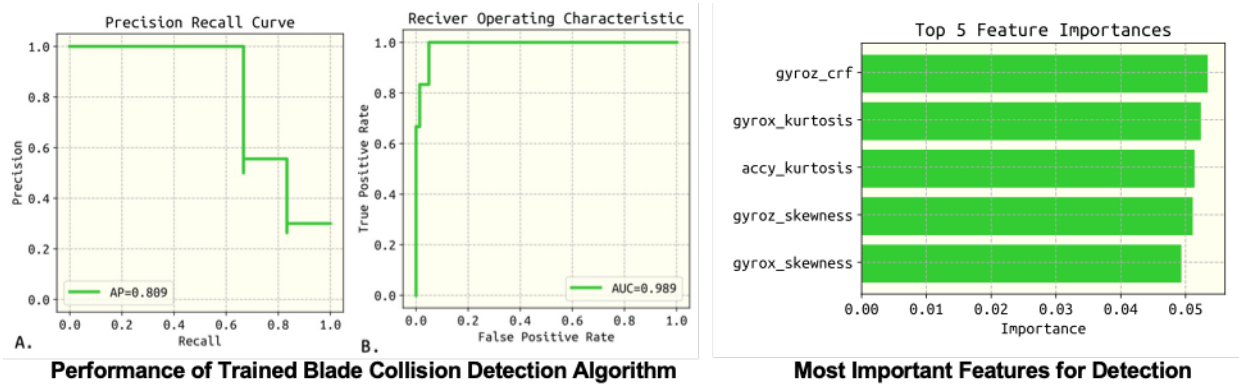


Figure 34. Performance of trained collision detection classifier on recorded multi-sensor turbine data collected during NREL-NWTC field testing, including precision and recall and the receiver operation characteristic (ROC); top five features (for driving classification) can be extracted from the forest-based model.

To generate features for classifier training, the signals were first separated into non-overlapping windows and labeled to contain either an on-blade collision or no collision. Multiple signal features were calculated for each window, including conventional statistical features such as root mean square, standard deviation, variance, kurtosis, and skewness, which were selected to extend prior work [14]. Machine learning techniques for structural health monitoring in wind turbine blades [15] have additionally shown crest factor, impulse factor, and RMS entropy estimator to be effective in determining anomalous vibration activity from background noise and were also included. Calculated feature vectors were then normalized using a z-score normalization, and the data was then separated into a 0.25/0.75 test-train split; a total of 1161 1.5s time windows (870 for training, 291 for testing) were used. The AdaBoost random forest ensemble algorithm was then trained on the data using SciKitLearn [16], [17].

The classifier was evaluated using a receiver operating characteristic curve (ROC) and a precision recall curve (PRC) and are shown in **Fig. 34**. In these results, the area under the curve (AUC) for the classifier is 0.989, but due to the rarity of a collision for the system the PRC was used to more accurately express the classifier accuracy with a large class imbalance. The average precision (AP) for the system is found to be 0.809.

A further benefit of using a forest-based model is the ability to rank the input features in terms of importance. The top 5 features in terms of AdaBoost vote weighting are shown in **Fig. 34**, which include z-axis gyrometer crest factor, x-axis gyrometer kurtosis, y-axis accelerometer kurtosis, and both z-axis and x-axis gyrometer skewness. In future work, this may lead to a reduced complexity for a real-time inference engine operating on a minimum number of input features.

Summary of findings

Final field testing at NREL-NWTC demonstrate successful operation of the complete, integrated eagle detection and deterrent system, including 360° imaging from the nacelle, on-blade multi-sensor data recording and image capture across turbine operations and surrogate blade strikes, and remote triggering of the kinetic visual deterrent system. The eagle classification algorithm was not included in this testing. Following the field test, the multi-sensor data recordings allowed for additional collision detection algorithm development, in which training and testing of machine learning classifiers can be performed *in silico* using real-world recorded on-blade sensor data, enabling continued and iterative improvement and validation of the complete system performance.

4. Conclusions and Suggested Future Work

A focus of this project was to extend prior efforts in the development of an on-blade collision sensor system for wind turbines to provide a coordinated visual detection, visual deterrent, and blade-strike collision detection system for golden eagles. Specific enhancements to hardware and software systems provide the following added functionality and identified challenges:

4.1. Automated Visual Detection of Eagles:

As described in Section 2.1, a machine learning approach was used to develop an automated classifier algorithm for eagle detection in images or video streams, in particular from a 360° 4K camera. Classifier training and testing was conducted using videos collected in the field of trained raptors, including both eagles and non-eagles. Following iterative improvement of the system, the classifier demonstrated up to 91.54% per-frame accuracy for classifying eagles using field-recorded videos from the 360° camera. While successful for eagle detection, this development revealed a few challenges worth consider for future work. First, while 4K represents state-of-the-art resolution for consumer field-ready cameras, this resolution spread over 360° viewing limits the overall system visual acuity. As such, birds recorded beyond approximately 150ft from the camera could not be distinguish as eagle vs. non-eagle raptor even by human eye. For longer-range detection, an array of non-360° cameras (e.g. four cameras pointed orthogonally at the horizon, and one point up) would provide additional visual acuity and could leverage the same classification approach. Second, preparing or acquiring training videos presents a unique challenge, as it may be infeasible to gather sufficient eagle and non-eagle video under conditions similar to wild eagle behavior near constructed wind turbines. Similarly, *in situ* testing of eagle detection performance may be infeasible outside of a long-term installed test.

4.2. Visual Deterrent using Kinetic Humanoid Devices:

As described in Section 2.2, a visual deterrent system was developed that used the remote, automated deployment of large (10-20ft) inflatable ‘air dancer’ devices used commonly for commercial advertising applications, as ground-based human activity is one of few verified eagle deterrent strategies. The devices were tested for use in the field, including under high-wind conditions and using accelerated lifetime materials testing. Two small field trials (3-5 days each) were conducted to test the efficacy of the visual deterrent at altering the flight trajectory of wild eagles. As described in the report, overall results of this testing are inconclusive due to the small number (< 5 per day) of eagle interactions, despite targeting field test areas with known eagle populations. This illustrates the difficulty of verifying deterrent efficacy in wild eagle populations, and a much longer or larger field trial would be required to prove or disprove efficacy of the approach.

4.3. Automated Blade-Strike Collision Detection:

As described in Section 2.3, a multi-sensor on-blade electronics module was developed and demonstrated, which includes a 3-axis accelerometer, 3-axis gyrometer, blade surface contact microphone, and down-blade camera mounted near the root of each wind turbine blade. On-board computation provides continuous, real-time data acquisition from all sensors, and automated collision detection is used to save a video of objects striking the blade. Control and

data acquisition are provided wirelessly for each blade root sensor module. Over three field tests (Section 3.1-3.3), the modules were successfully used to detect and capture images of blade strikes using surrogate projectiles (e.g. tennis balls). While successful for ~60g surrogate objects and thereby likely sufficient for detecting golden eagle strikes (3-5 kg), future work may add additional and/or distributed sensors (contact microphones or accelerometers) along the blade length to increase sensitivity and provide collision detection (and possibly localization) for smaller striking objects, such as smaller birds or bats.

4.4. Ongoing Work using Recorded Data Sets from On-Turbine Testing:

As described in Section 3.4, the multiple on-turbine field tests (Section 3.1-3.3) provide a rich multi-sensor data set than can be used offline for continued analysis of on-turbine sensor noise and sensor sensitivity, as well as continued development and testing of automated detection algorithms. This is expected to support ongoing *in silico* development, enabling iterative improvement and validation in advance of future field testing.

5. Summary of Project Outcomes (Task 6.0)

5.1. Presentations

Conference Presentations

- Albertani, R., Clocker, K., Davis, C., Johnston, M., Vang, J., “Autonomous Eagle Smart Detection, Ground Deterrent and Blade-Event Monitoring,” *Wind Wildlife Research Meeting XIII*, Virtual, Dec 1-4, 2020.
- Clocker, K., Hu, C., Albertani, R., and M.L. Johnston, "Sensor System and Signal Processing for Automated Blade Collision Detection on Wind Turbines", *IEEE SENSORS 2020*, Rotterdam, Netherlands (Virtual).
- Albertani, R., Clocker, K., Hu, C., Johnston, M., “Automatic Intelligent Eagle Detection, Deterrent and Blade-Event Monitoring,” *Wind Europe Offshore 2019*, Copenhagen, Nov 26 - 28, 2019.
- Albertani, R., Johnston, M., Todorovic, S., Huso M., Katzner, T., “Eagle Detection, Identification and Deterrent, with Blade Collision Detection for Wind Turbines,” *Wind Wildlife Research Meeting XII*, St Paul, MN, Nov 27 - Nov 30, 2018.
- Maurer, W., Albertani, R., “Eagle Detection, Interaction Sensing, and Deterrence System for Wind Turbines,” *AIAA Region VI Student Conference*, UC Merced, Merced, CA, April 6-8, 2018. *2nd Place Best Student Paper*
- Albertani, R., Johnston, M., Todorovic, S., Huso M., Katzner, T., “A System for Eagle Detection, Deterrent and Collision-Detection for Wind Turbines,” *National Wind Coordinating Collaborative Webinar*, Webinar Presentation, May 19th, 2017

Invited Presentations

- Albertani, R., “Help Wildlife Coexist with Wind Energy Deployment,” Department of Earth Sciences, Section of Wind Energy, Uppsala Universitat, Gotland Campus, November 30th, 2019.
- Kyle Clocker, Congcong Hu, Matthew Johnston, and Roberto Albertani, “Automated System for Eagle Detection, Deterrent, and Wildlife Collision Detection for Wind Turbines,” *WETO Wind Wildlife Training Meeting*, NWTC, Boulder, CO, Sept. 18, 2019.

- Albertani, R., “Help Eagles Coexist with Wind Energy Deployment,” Birders' Night, East Cascades Audubon Society, Bend, OR, November 15th, 2018.
- Albertani, R., “Reducing the Impacts of Wind Energy on Raptors,” Birder’s Night Meeting, Salem Audubon Society, Salem, OR, October 9th, 2018.
- Albertani, R., “Blade-Strike and Birds Detection for Offshore Wind Turbines,” California Offshore Renewables Environmental Regulatory Workshop, Sacramento, CA, March 14th, 2018.
- Albertani, R., “Addressing Wind Energy-Eagle Interactions (with Engineering),” Thursday Nights Lectures Series, High Desert Museum, Bend, OR, January 25th, 2018.

5.2. Peer-Reviewed Publications / Proceedings

- Hu, C., Albertani, R., “Wind turbine event detection by support vector machine,” (*In Review*).
- Clocker, K., Hu, C., Albertani, R., and M.L. Johnston, “Sensor System and Signal Processing for Automated Blade Collision Detection on Wind Turbines”, *IEEE SENSORS 2020*, pp. 1-5, 2020.
- Hu, C., Albertani, R., “Machine Learning applied to wind turbine blades impact detection,” *Wind Engineering*, May 2019, <https://doi.org/10.1177/0309524X19849859>.
- Hu, C., Albertani, R., Suryan, R. M., “Wind turbine sensor array for monitoring avian and bat collisions,” *Wind Energy*, DOI: 10.1002/we.2160, January 2018.

5.3. Intellectual Property

- Albertani, R., Maurer, W., Johnston, M., Clocker, K., Hu, C., “Apparatus and amendment of wind turbine blade impact detection and analysis,” U.S. Patent App. 16/741,638.

5.4. Demonstrations

- Kyle Clocker, Congcong Hu, Matthew Johnston, and Roberto Albertani, “Automated System for Eagle Detection, Deterrent, and Wildlife Collision Detection for Wind Turbines,” *WETO Wind Wildlife Training Meeting*, NWTC, Boulder, CO, Sept. 18, 2019.

5.5. Media

- Live interview during eagle flight tests by Zolo Media for KOHD-KBNZ network, Oregon
- Interviews, articles or web publication on the project for CCTV News, The Corvallis Advocate, Digital Trends, News Channel 21 KTVZ, Science Daily, Discovery Channel Canada.
- The Corvallis Advocate (<http://www.corvallisadvocate.com/2017/renewable-energy-fewer-casualties/>)
- Interview on KGW News (<https://www.youtube.com/watch?v=0ohH-6Ftg2g>)
- KTVZ News Channel 21 (<https://www.ktvz.com/news/osu-research-aims-to-protect-eagles-from-wind-turbines/477684361>)
- Albany Democrat-Herald Corvallis Gazette (see Appendix B)
- Interview with The Wildlife^[SEP]Society's
- Live interview with Central Oregon Daily News (<http://zolomedia.com/osu-researcher-trying-prevent-deaths-eagles-hit-wind-turbines/>)
- Bend (OR) Bulletin (<https://www.bendbulletin.com/home/6303536-151/high-desert-museums-eagles-help-osu-researchers>)
- EurekAlert (https://www.eurekalert.org/pub_releases/2018-03/osu-dds031918.php)

- Publication of the project on Oregon State University MIME Bulletin and Momentum (<https://mailchi.mp/engineering.oregonstate.edu/momentum-newsletter-3266649>)
- Other miscellaneous:
- <https://www.labroots.com/trending/technology/8354/smart-wind-turbines-reduce-eagles-deaths>
- <http://dailycaller.com/2018/06/17/researchers-spend-625000-turbines/>
- <https://apnews.com/52c58b68dfa844ed926511f45c7190b4>
- <https://www.kentucky.com/news/business/article213336764.html>
- Oregon Live – Associate Press “Eagles teach Oregon researchers how to stop wind turbines from killing raptors”
- Ebmag, “Cameras and ‘thump’ sensor research to protect eagles from wind turbines,” <https://www.ebmag.com/renewables/cameras-and-thump-sensor-research-to-protect-eagles-from-wind-turbines-19713>

6. Acknowledgments

We are greatly indebted to our collaborators at the National Renewable Energy Laboratory’s National Wind Technology Center and the Mesaland Community College’s North American Wind Research and Training Center at Meslands Community College. We also thank all of the science, management, and industry representatives who willingly shared their knowledge and feedback throughout the project, with special thanks to Manuela Huso, Todd Katzner, and Bryce Robinson. We thank Department of Energy program managers and grant administrators for their guidance and support of this project.

7. References

1. T.D.Allison,J.E.Diffendorfer,E.F.Baerwald,J.A.Beston,D.Drake, A. M. Hale, C. D. Hein, M. M. Huso, S. R. Loss, J. E. Lovich *et al.*, “Impacts to wildlife of wind energy siting and operation in the united states,” *Issues in Ecology*, vol. 21, pp. 1–24, 2019.
2. E.B.ArnettandR.F.May,“Mitigatingwindenergyimpactsonwildlife: approaches for multiple taxa,” *Human–Wildlife Interactions*, vol. 10, no. 1, p. 5, 2016.
3. R. May, A. B. Gill, J. Ko ¨ppel, R. H. Langston, M. Reichenbach, M. Scheidat, S. Smallwood, C. C. Voigt, O. Hu ¨ppop, and M. Portman, “Future research directions to reconcile wind turbine–wildlife interac- tions,” in *Wind Energy and Wildlife Interactions*. Springer, 2017, pp. 255–276.
4. K. C. Sinclair, “Approaches to addressing environmental challenges with wind energy in the united states,” National Renewable Energy Lab.(NREL), Golden, CO (United States), Tech. Rep., 2017.
5. Matchett, M. R., O’Gara, B. W., “Methods of Controlling Golden Eagle Depredation on Domestic Sheep in Southwestern Montana,” *The Journal of Raptor Research*, 21(3): 85-94, 1987.
6. Sinclair, K., DeGorge, E., “Wind Energy Industry Eagle Detection and Deterrents: Research Gaps and Solutions Workshop Summary Report,” National Renewable Energy Laboratory (NREL), Technical Report NREL/TP-5000-65735, April 2016.
7. Telenko, D., et al., “Evaluation of Novel Bird Repellants in Vegetable Crops,” Sustainable Agriculture Research & Education, Cornell University, 2015 Annual Report.
8. “Air Dancers as a Potential Bird Deterrent in Blueberries”, College of Agricultural Sciences, Cornell University, New York Berry News, Volume 13, Njmbner 4, May 30, 2014.

9. Clocker, K., Hu, C., Albertani, R., and M.L. Johnston, "Sensor System and Signal Processing for Automated Blade Collision Detection on Wind Turbines", *IEEE SENSORS 2020*, Rotterdam, Netherlands (Virtual).
10. L.Rademakers,E.Wiggelinkhuizen,S.Barhorst,andH.deBoon,"Bird collision monitoring system for multi megawatt wind turbines wt bird prototype development and testing," ECN, Tech. Rep., 2006.
11. Y. Freund and R. E. Schapire, "A decision-theoretic generalization of on-line learning and an application to boosting," in *European conference on computational learning theory*. Springer, 1995, pp. 23–37.
12. L. Breiman, "Random forests," *Machine learning*, vol. 45, no. 1, pp. 5–32, 2001.
13. Y. Freund, R. Schapire, and N. Abe, "A short introduction to boosting," *Journal-Japanese Society For Artificial Intelligence*, vol. 14, no. 771- 780, p. 1612, 1999.
14. C. Hu and R. Albertani, "Machine learning applied to wind turbine blades impact detection," *Wind Engineering*, p. 0309524X19849859, 2019.
15. J. Solimine, C. Niezrecki, and M. Inalpolat, "An experimental investigation into passive acoustic damage detection for structural health monitoring of wind turbine blades," *Structural Health Monitoring*, vol. 0, no. 0, p. 1475921719895588, 0. [Online]. Available: <https://doi.org/10.1177/1475921719895588>
16. T. Hastie, S. Rosset, J. Zhu, and H. Zou, "Multi-class adaboost," *Statistics and its Interface*, vol. 2, no. 3, pp. 349–360, 2009.
17. F. Pedregosa, G. Varoquaux, A. Gramfort, V. Michel, B. Thirion, O. Grisel, M. Blondel, P. Prettenhofer, R. Weiss, V. Dubourg, J. Vander- plas, A. Passos, D. Cournapeau, M. Brucher, M. Perrot, and E. Duchesnay, "Scikit-learn: Machine learning in Python," *Journal of Machine Learning Research*, vol. 12, pp. 2825–2830, 2011.
18. N. Johnston, J. Bradley, K. Otter, "Increased Flight Altitudes among Migrating Golden Eagles Suggest Turbine Avoidance at a Rocky Mountain Wind Installation," *PLOS ONE* 9(3): e93030, 2014.